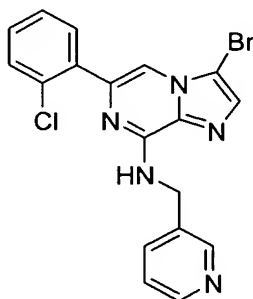


REMARKS

Claims 1-30 are pending in the Application. On March 9, 2004, the Examiner telephoned the undersigned Attorney-of-Record and requested the election of a species for prosecution purposes; no division into Groups was communicated. Applicants elected the following species, with traverse, to comply with the Examiner's requirement:



The present Office Action correctly identifies the elected species. Applicants affirm the election of the species with traverse.

Furthermore, in the present Office Action, the Examiner states that since the "elected species was not found in the prior art search and as per the guidelines..., the examination was expanded to compounds of **formula III wherein R³ is (pyridyl)methyl and R² is as defined in the claims while retaining the definitions of R and R¹ as in the elected species...**" (Page 4 of the Office Action). The Examiner withdrew Claims 3-4, 9, and 13-16 from further consideration as being drawn to non-elected species. Also withdrawn from consideration were "[a]ll other definitions of the variables R, R¹, and R³ from the generic claims 1-2, 5-8, 10-12 and 19-30, and the species from claims 17-18 that do not fall in the above-described subgenus....as being drawn to non-elected subject matter." (Pages 4-5 of the Office Action).

Applicants respectfully request reconsideration of the restriction by the Examiner. Applicants believe that all claims 1-30, as filed, form part of one and the same invention. Applicant believes that when there is a linking claim (e.g., Claim 1) encompassing the scope of all the processes, compounds etc., it is inappropriate to restrict the invention into these various inventions. Applicant also believes that due to such commonality, a complete examination of claims 1-30 would not cause undue burden. Applicant further believes that

the same art search will most probably apply to the alleged separate inventions, and respectfully submit that the restriction is improper.

Under the statute "two or more independent and distinct inventions.... in one application may.... be restricted to one of the inventions." Inventions are "independent" if "there is no disclosed relationship between two or more subjects disclosed" (MPEP 802.01). The term "distinct" means that "two or more subjects as disclosed are related.... but are capable of separate manufacture, use or sale as claimed, and are patentable over each other" (MPEP 802.01). However, even when patentably distinct inventions, restriction is not required unless one of the following reasons appear (MPEP 808.02):

1. Separate classification
2. Separate status in the art; or
3. Different field of search.

In the present application, Applicants believe that the Examiner has not established a clear reason to establish the existence of any of the above 1-3 situations. Reconsideration and withdrawal of the restriction requirement are, therefore, respectfully requested.

In any case, Applicants preserve the right to pursue the scope of any non-elected claims later by divisional applications if Applicants choose to do so.

While appreciative of the Examiner's inclusion of the definition of R² as defined in the claims for prosecution, Applicants specifically wonder why only the "(pyridyl)methyl" has been included in the definition for R³ and only the "2-chlorophenyl" has been included in the definition for R. Applicants believe that the other moieties, or at least other similar moieties, should also be included for R and R³ for prosecution purposes which would indeed bring the withdrawn claims 3-4, 9 and 13-16, withdrawn subject matter of claims 1-2, 5-8, 10-12 and 19-30, and the withdrawn species from claims 17-18, or some of that, into prosecution. Applicants respectfully request such a consideration by the Examiner.

While the above-noted request is pending, Applicants are addressing the objection and rejections of claims that the Examiner has raised in the claims that are currently under prosecution based on the instant Office Action.

Claim 18 was found allowable.

The specification was objected to on the grounds that several structural formulae in Table 4 on pages 50-56 were not completely legible. Replacement pages were required. Applicants are supplying the replacement pages herewith.

Claims 19-20, 22-23 and 25-27 were rejected under 35 U.S.C. § 112, first paragraph, on enablement grounds. The Examiner stated that the specification "while enabling for a method of inhibiting CDK2 and/or a method of treatment of specific cancers (recited in claim 24), does not reasonably provide enablement for inhibiting all types of cyclin dependent kinases or for the treatment of all other diseases embraced by the instant claims." (Pages 5-6 of the Office Action). Applicants believe that the **Background of the Invention** provides sufficient enablement for linking CDK2 with other cyclin dependent kinases and the various diseases. However, in the interest of furthering the prosecution, Applicants have now amended claims 19-20 and 25 and cancelled claims 21-23. Applicants believe that this amendment should satisfy the Examiner's concerns. Applicants, however, would like to emphasize that the amendment should not be perceived as an admission that the cancelled or given-up scope of the claims is not patentable. Applicants preserve the right to pursue such scope later by divisional applications if Applicants choose to do so.

Claims 25-27 were rejected under 35 U.S.C. § 112, second paragraph, as being indefinite for lack of antecedent basis for the phrase "or a pharmaceutically acceptable salt or solvate thereof". Claim 1, from which claim 25 depends, has now been amended to include that phrase. Support for this occurs on page 3, line 24 of the specification. Withdrawal of the 35 U.S.C. § 112 rejection is, therefore, respectfully requested.

Claims 1-2, 5-8, 10-12, 17 and 19-30 were rejected under 35 U.S.C. § 103(a) as being obvious over Burns *et al*, WO 02/060492. The '492 publication discloses certain pyrazines. As the Examiner points out, the reference compounds lack a substitution in the (present) R² position. The Examiner states: "Since the instant compounds differ by having a methyl group in place of the hydrogen disclosed for reference compounds (i.e., differing by a CH₂ group), the instantly claimed compounds are homologs of

the reference compound. One having ordinary skill in the art would have been motivated to prepare the instantly claimed compounds because such structurally homologous compounds would be expected to possess similar utilities. " (Page 10 of the Office Action). Applicants would respectfully like to disagree with the Examiner's contention. The instantly claimed compounds are structurally dissimilar from the reference's teaching and their structures or synthesis are not taught by the reference. Additionally, pharmaceutical art is notoriously unpredictable. Any changes in the structure of a molecule may so drastically and significantly change the biological activity that the prediction of the utilities becomes impossible. This fact is well known in the art. Applicants are enclosing two articles to illustrate this point:

1st illustration (EXHIBIT A): Applicants would like to bring to the attention of the Examiner the attached copy of C. Breitenlechner *et al*, *Structure*, 11, 1595-1607 (December 2003), with relevant passages highlighted. The article compares two kinase inhibitors (H-1152P and HA-1077) whose structures shown on page 1596 differ only as methyl versus non-methyl compounds. As the article clearly shows, the methyl compound H-1152P shows a 200-fold increase in inhibitory activity and also a 40- to 100-fold increase in selectivity, when compared to the non-methyl analog, HA-1077.

2nd illustration (EXHIBIT B): Yet another evidence to the same effect is provided by R. Capdeville *et al*, *Nature Reviews*, 1, 493-502 (July 2002). The authors, all from Novartis Pharmaceuticals (the makers of the commercial anti-cancer compound Glivec[®]) discuss (on page 494, left column, marked part) the activity of a methyl-substituted compound (structure **c** in Fig. 1) with its non-methyl analog (structure **b** in Fig. 1). The authors state: " At this point, a key observation from analysis of structure-activity relationships was that a substitution at position 6 of the diaminophenyl ring **abolished PKC inhibitory activity completely**. Indeed, although the introduction of a simple 'flag-methyl' led to loss of activity against PKC, the activity against protein tyrosine kinases was retained or even enhanced... " (emphasis added). Thus, as the authors note, the substitution of a methyl for a H abolished the PKC inhibitory activity completely. Applicants submit that owing to such unpredictable nature of biological activity, neither the instant compounds nor their utilities can be



predicted from the cited art, and, therefore, the instant claims cannot be considered to be obvious over the art cited. Withdrawal of the 35 U.S.C. § 103(a) rejection is, therefore, respectfully requested.

Claim 30 was objected to by the Examiner; it is now cancelled.

- 5 There being no other rejections pending, Applicants believe that the claims, as amended, are in allowable condition and such an action is earnestly solicited. If the Examiner has any questions, the Examiner is invited to contact the undersigned.

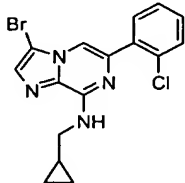
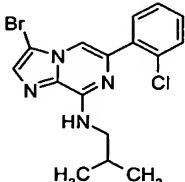
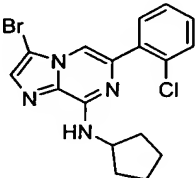
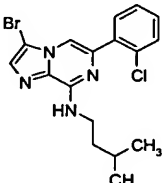
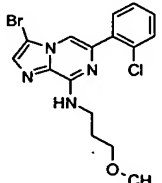
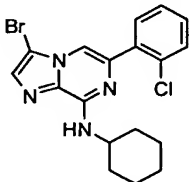
March 29, 2004
Schering-Plough Corporation
2000 Galloping Hill Road
Patent Department, K-6-1, 1990
Kenilworth, NJ 07033
Tel: (908) 298-5068
Fax: (908) 298-5388

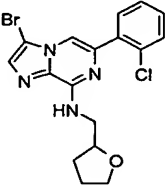
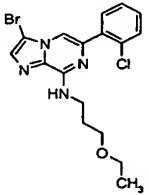
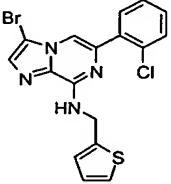
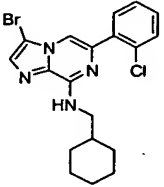
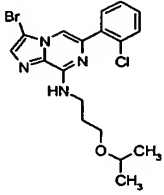
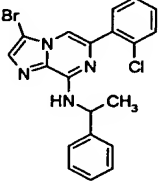
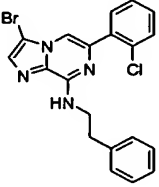
Respectfully submitted,

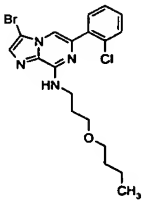
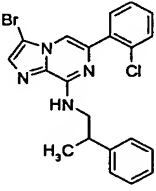
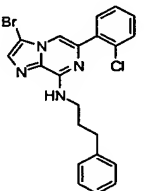
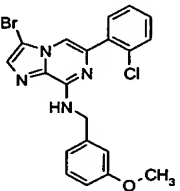
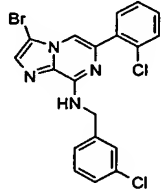
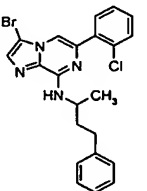
A handwritten signature in black ink, appearing to read "Dr. Palaiyur S. Kalyanaraman".

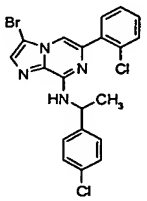
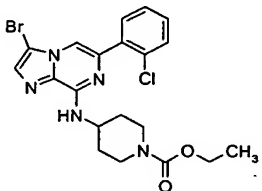
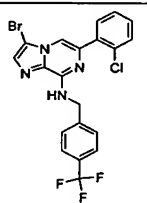
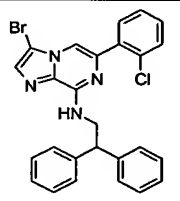
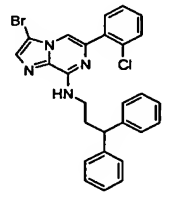
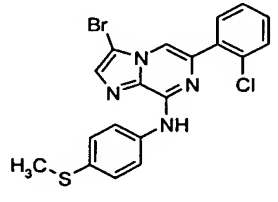
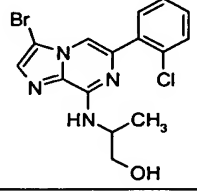
Dr. Palaiyur S. Kalyanaraman
Attorney for Applicants
Reg. No. 34,634

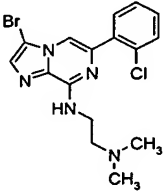
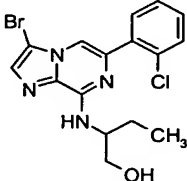
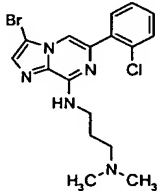
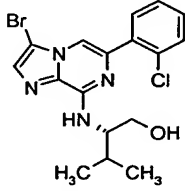
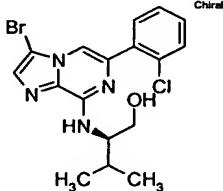
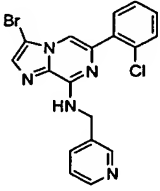
TABLE 4

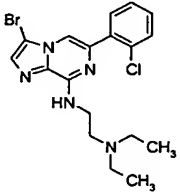
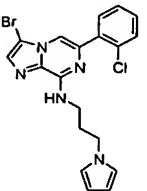
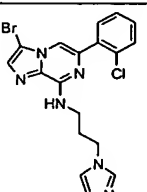
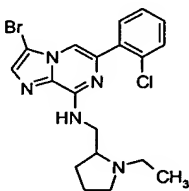
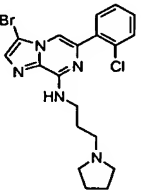
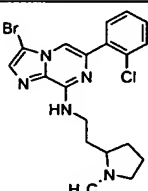
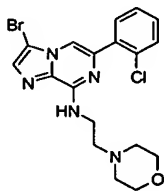
	STRUCTURE	MW	LCMS m/z	% PURITY
	 <chem>Nc1nc2nc(Br)cnc2n1-c3ccccc3ClC4CC4</chem>	377.7	379.2	97
	 <chem>CC(C)CNc1nc2nc(Br)cnc2n1-c3ccccc3Cl</chem>	379.7	381.2	90
	 <chem>Nc1nc2nc(Br)cnc2n1-c3ccccc3ClC4CCCC4</chem>	391.7	393.2	93
	 <chem>CC(C)CCNc1nc2nc(Br)cnc2n1-c3ccccc3Cl</chem>	393.7	395.2	99
	 <chem>COCCCNc1nc2nc(Br)cnc2n1-c3ccccc3Cl</chem>	395.7	397.1	98
	 <chem>Nc1nc2nc(Br)cnc2n1-c3ccccc3ClC4CCCCC4</chem>	405.7	407.1	100

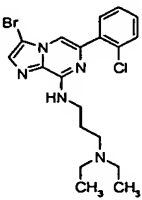
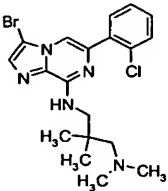
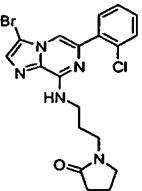
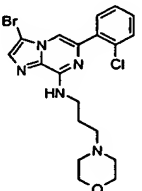
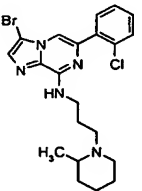
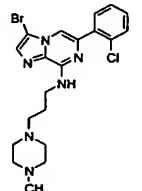
	 <chem>BrC1=CN=C(NC2CCOC2)N=C1C3=CC=CC=C3Cl</chem>	407.7	409.2	93
	 <chem>BrC1=CN=C(NCCOCC)N=C1C2=CC=CC=C2Cl</chem>	409.7	411.2	99
	 <chem>BrC1=CN=C(NCC2=CC=CS2)N=C1C3=CC=CC=C3Cl</chem>	419.7	421.1	100
	 <chem>BrC1=CN=C(NCC2CCCCC2)N=C1C3=CC=CC=C3Cl</chem>	419.8	421.2	94
	 <chem>BrC1=CN=C(NCCOC(C)C)N=C1C2=CC=CC=C2Cl</chem>	423.7	425.2	100
	 <chem>BrC1=CN=C(NC(C)c2ccccc2)N=C1C3=CC=CC=C3Cl</chem>	427.7	429.2	99
	 <chem>BrC1=CN=C(NCCc2ccccc2)N=C1C3=CC=CC=C3Cl</chem>	427.7	429.2	91

	 <chem>BrC1=CN2=C(NC(=N2)C3=CC=CC=C3Cl)C=NC4=CC=CC=C4OCCOC</chem>	437.8	439.2	95
	 <chem>BrC1=CN2=C(NC(=N2)C3=CC=CC=C3Cl)C=NC4=CC=CC=C4C(C)C5=CC=CC=C5</chem>	441.8	443.2	90
	 <chem>BrC1=CN2=C(NC(=N2)C3=CC=CC=C3Cl)C=NC4=CC=CC=C4CCc5ccccc5</chem>	441.8	443.2	94
	 <chem>BrC1=CN2=C(NC(=N2)C3=CC=CC=C3Cl)C=NC4=CC=CC=C4COc5ccccc5</chem>	443.7	445.1	100
	 <chem>BrC1=CN2=C(NC(=N2)C3=CC=CC=C3Cl)C=NC4=CC=CC=C4Cc5cc(Cl)ccc5</chem>	448.2	449.1	91
	 <chem>BrC1=CN2=C(NC(=N2)C3=CC=CC=C3Cl)C=NC4=CC=CC=C4C(C)Cc5ccccc5</chem>	455.8	457.3	99

	 <chem>CC(Nc1nc2nc(Br)nc2n1-c1ccc(Cl)cc1)c3ccc(Cl)cc3</chem>	462.2	463.1	99
	 <chem>CCOC(=O)N1CCCN(C1Nc2nc3nc(Br)nc3n2-c4ccc(Cl)cc4)CC1</chem>	478.8	480.1	100
	 <chem>FC(F)(F)c1ccc(CNc2nc3nc(Br)nc3n2-c4ccc(Cl)cc4)cc1</chem>	481.7	483.3	97
	 <chem>CC1(Cc2nc3nc(Br)nc3n1-c4ccc(Cl)cc4)c5ccccc5</chem>	503.8	505.1	94
	 <chem>CC1(Cc2nc3nc(Br)nc3n1-c4ccc(Cl)cc4)c5ccccc5</chem>	517.9	519.1	100
	 <chem>CS(=O)c1ccc(Nc2nc3nc(Br)nc3n2-c4ccc(Cl)cc4)cc1</chem>	445.8	447.2	98
	 <chem>CC(O)Nc1nc2nc(Br)nc2n1-c3ccc(Cl)cc3</chem>	381.7	383.1	99

	 <chem>CN(C)CCNC1=NC2=C(N1)N=CN=C2C3=CC=CC=C3Cl</chem>	394.7	396.2	98
	 <chem>CCOCCNC1=NC2=C(N1)N=CN=C2C3=CC=CC=C3Cl</chem>	395.7	397.1	92
	 <chem>CN(C)CCCN1=NC2=C(N1)N=CN=C2C3=CC=CC=C3Cl</chem>	408.7	410.2	98
	 <chem>CC(C)C(O)CCNC1=NC2=C(N1)N=CN=C2C3=CC=CC=C3Cl</chem>	409.7	411.1	100
	 <chem>CC(C)C(O)CCNC1=NC2=C(N1)N=CN=C2C3=CC=CC=C3Cl</chem> Chiral	409.7	411.2	96
	 <chem>c1cccnc1CN1=NC2=C(N1)N=CN=C2C3=CC=CC=C3Cl</chem>	414.7	416.1	97

	 <chem>CCN(CC)CCNC1=NC2=C(N1)N=CN=C2C3=CC=CC=C3Cl</chem>	422.8	424.2	98
	 <chem>C1=CC=C(C=C1)NCCNC2=NC3=C(N2)N=CN=C3C4=CC=CC=C4Cl</chem>	430.7	432.2	94
	 <chem>C1=CC=C(C=C1)N1C=CN=C1CCNC2=NC3=C(N2)N=CN=C3C4=CC=CC=C4Cl</chem>	431.7	433.2	94
	 <chem>CCN1CCCC1CCNC2=NC3=C(N2)N=CN=C3C4=CC=CC=C4Cl</chem>	434.8	436.1	100
	 <chem>C1=CC=C(C=C1)N1CCCC1CCNC2=NC3=C(N2)N=CN=C3C4=CC=CC=C4Cl</chem>	434.8	436.1	100
	 <chem>CN1CCCC1CCNC2=NC3=C(N2)N=CN=C3C4=CC=CC=C4Cl</chem>	434.8	436.2	95
	 <chem>C1CN(CCC1)CCNC2=NC3=C(N2)N=CN=C3C4=CC=CC=C4Cl</chem>	436.7	438.1	100

		436.8	438.2	98
		436.8	438.2	98
		448.8	450.2	95
		450.8	452.2	95
		462.8	464.3	99
		463.8	465.3	92

Protein Kinase A in Complex with Rho-Kinase Inhibitors Y-27632, Fasudil, and H-1152P: Structural Basis of Selectivity

Christine Breitenlechner,¹ Michael Gaßel,²
Hiroyoshi Hidaka,⁴ Volker Kinzel,²
Robert Huber,¹ Richard A. Engh,^{1,3,*}
and Dirk Bossemeyer^{2,*}

¹Abteilung Strukturforschung
Max-Planck-Institut fuer Biochemie
82152 Martinsried

²Department for Pathochemistry
German Cancer Research Center
69120 Heidelberg

³Department of Medicinal Chemistry
Roche Diagnostics GmbH
82372 Penzberg
Germany

⁴D-Western Therapeutics Institute
Yagota Building 2C
100-32 Yagotohonmachi
Showa-ku, Nagoya 466 0825
Japan

Summary

Protein kinases require strict inactivation to prevent spurious cellular signaling; overactivity can cause cancer or other diseases and necessitates selective inhibition for therapy. Rho-kinase is involved in such processes as tumor invasion, cell adhesion, smooth muscle contraction, and formation of focal adhesion fibers, as revealed using inhibitor Y-27632. Another Rho-kinase inhibitor, HA-1077 or Fasudil, is currently used in the treatment of cerebral vasospasm; the related nanomolar inhibitor H-1152P improves on its selectivity and potency. We have determined the crystal structures of HA-1077, H-1152P, and Y-27632 in complexes with protein kinase A (PKA) as a surrogate kinase to analyze Rho-kinase inhibitor binding properties. Features conserved between PKA and Rho-kinase are involved in the key binding interactions, while a combination of residues at the ATP binding pocket that are unique to Rho-kinase may explain the inhibitors' Rho-kinase selectivity. Further, a second H-1152P binding site potentially points toward PKA regulatory domain interaction modulators.

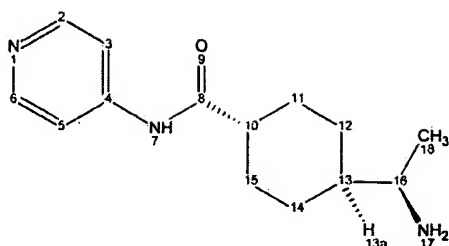
Introduction

Protein kinases are phosphorylation enzymes that control cellular signaling events and accordingly may cause a wide range of diseases when defective. Since they are typically active only when signaling, most of the diseases associated with protein kinase deregulation (including the majority of all cancers) arise from excess activity due to mutation, overexpression, or disabled cellular inhibition. Other protein kinases contribute to disease in the course of their normal function in cellular

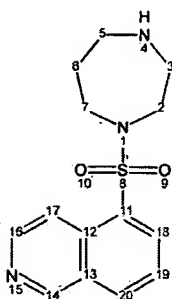
processes such as cell survival or cell migration. The prevalence of kinases to cause or augment disease underscores the need for therapeutic protein kinase inhibitors, with the caveat that they must be highly selective for their dysregulated targets to avoid inhibition of other ubiquitous but essential protein kinases. Several protein kinase inhibitors have been approved for human treatment or are in advanced clinical trials. The first was fasudil (HA-1077 or AT877), which was approved in 1995 for the treatment of cerebral vasospasm, a painful and potentially deadly result of subarachnoid hemorrhage. Fasudil has significant vasodilatory activity (Ono-Saito et al., 1999) and is now undergoing clinical trials for the treatment of angina pectoris (Shimokawa et al., 2001). Fasudil's activity has been attributed to inhibition of Rho-kinase (Matsui et al., 1996) and its role in signaling for myosin light chain phosphorylation and arterial smooth muscle contraction (Amano et al., 1996), although the *in vitro* activity of fasudil is not strictly limited to Rho-kinase. Other Rho-kinase-related protein kinases, such as PKA, PRK2, MSK1, and S6K1, are also inhibited by fasudil, although to a lesser extent (Davies et al., 2000). Fasudil is related to H7, an isoquinoline sulfonamide derivative that is a weak PKC inhibitor (Hidaka et al., 1984) and whose protein kinase binding mode was shown by the cocrystal structure with PKA (Engh et al., 1996). Fasudil has a heptameric homopiperazine ring at the position of the methyl-piperazine ring of H7 (Figure 1). Further derivitization of fasudil led to H-1152P, with two additional methyl groups, one at the isoquinoline ring and the other at the homopiperazine ring (Tanaka et al., 1998). H-1152P has a better inhibitory profile than HA-1077, with a K_D value for Rho-kinase in the low nanomolar range and a reportedly enhanced selectivity (Tanaka et al., 1998; Sasaki et al., 2002). Rho-kinase may be an important pharmacological target also for cancer because of its role in the phosphorylation of focal adhesion kinase (Sinnott-Smith et al., 2001) and the invasion and migration of cancer cells (for reviews, see Fukata et al., 2001; Amano et al., 2000). Regarding the latter, Itoh et al. (1999) showed that the migration of rat MM1 hepatoma cells was prevented by the Rho-kinase inhibitor Y-27632. As a pyridine derivative, Y-27632 differs in its chemical structure from H inhibitors described above. It has a K_D of 140 nM for Rho-kinase and 25 μ M for PKA (Ishizaki et al., 2000) and is ATP competitive, like the H inhibitors (Trauger et al., 2002; Ikenoya et al., 2002).

Crystal structure analyses of protein kinase inhibitor complexes reveal the intermolecular interactions responsible for ligand binding and thereby enable structure-based rational design and optimization of kinase inhibitors. To date, crystal structures have been determined for some 30 protein kinases, representing less than 6% of the 518 protein kinases in the human genome (Manning et al., 2002). Many of these structures have been complexes with protein kinase inhibitors, but most have shown an inactive state. As a serine-threonine kinase of the AGC group, Rho-kinase possesses a cata-

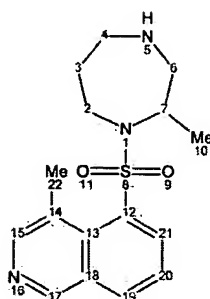
*Correspondence: d.bossemeyer@dkfz.de (D.B.), engh@biochem.mpg.de (R.A.E.)



Y-27632



HA-1077



H-1152P

Figure 1. Chemical Structures of the Inhibitors Y-27632, HA-1077, and H-1152P

lytic domain closely related to other AGC group kinases, among them PKA, PKB, PKC, and PKG, although no crystal structure of Rho-kinase has been reported. The close relationship between PKA and Rho-kinase and the well established crystallization conditions for PKA make PKA a suitable model system for studying Rho-kinase inhibitors. Furthermore, cocrystallization of PKA with Rho-kinase inhibitors helps identify factors governing cross selectivity of protein kinase inhibitors, a major concern in protein kinase inhibitor design.

The ATP binding site residues conserved between PKA and Rho-kinase include Phe327 (PKA numbering). This residue is a characteristic but not absolutely conserved feature of the AGC group of kinases. It is positioned on the C-terminal polypeptide strand which stretches between the α helical catalytic domain lobe and the C-terminal anchor in the hydrophobic motif. Phe327 shields one side of the ATP pocket and lies adjacent to the adenine of ATP and aromatic groups of ATP-site inhibitors (Prade et al., 1997; Engh et al., 1996). Rho-kinase and PKA differ, however, in eight positions in the ATP binding pocket (Figure 2). Four of their side chains are in close (<4 Å) contact with the inhibitors, corresponding to the following PKA→Rho substitutions: Leu49Ile, Val123Met, Thr183Ala, and Glu127Asp. Because the protein kinase fold is so highly conserved, variations of amino acid residues that line the ATP sub-site belong to the most important factors in defining inhibitor selectivity. Here we describe the crystal structures of PKA in complex with HA-1077 (at 2.2 Å resolution), with H-1152P (1.9 Å), and with Y-27632 (2.0 Å) and

analyze the factors governing their relative affinities for PKA and Rho-kinase. The structures identify the binding interactions of the inhibitors in the ATP pocket. The surface areas of the inhibitor/PKA interface correlate well with their inhibitory activities. Furthermore, the specific sequence differences between PKA and Rho-kinase provide an explanation for the observed higher affinity of these molecules for Rho-kinase. On the basis of these structural data, we propose models for the Rho-kinase-specific binding modes that rationalize the roles of the unique combination of amino acid residues found in the Rho-kinase ATP binding pocket. In addition, a second, well ordered H-1152P molecule was observed in a surface region with contact to the phosphoryl group of Thr197 and to Lys189, both from the activation loop, and to Glu86 from Helix C, a region critical for kinase activity and protein-protein interaction.

Results and Discussion

Overall Structure

The PKA complexes with Rho-kinase inhibitors Y-27632 (PKA-Y), fasudil or HA-1077 (PKA-1077), and H-1152P (PKA-1152) were cocrystallized as ternary complexes with the recombinant catalytic subunit of cyclic AMP-dependent protein kinase (PKA) and the pseudo-substrate kinase inhibitor peptide [PKI(5-24)]. All three inhibitor complexes crystallized in the orthorhombic space group P2₁2₁2₁. The PKA-1152 and PKA-Y crystals have similar cell constants (ca. 74.1, 76.6, 81.0) and the same crystal packing arrangement (Table 1). PKA-1077 has slightly different cell constants (70.33, 73.67, 79.08) and different crystal contacts. The inhibitor molecules occupy the ATP binding site; H-1152P binds additionally at a second site bounded by pThr197, helix C residues, and residues from the PKI(5-24) peptide of a symmetry related molecule. Apart from that, no direct contacts exist between any of the inhibitors and PKI(5-24).

Open and Closed Conformations

Ligand-induced conformational changes have been well documented for PKA (Prade et al., 1997; Johnson et al., 2001). Foremost among these are variations in the relative orientations of N- and C-terminal lobes, whose interface creates the ATP binding pocket. The "openness" of the pocket ranges from "closed" for PKA structures with bound ATP or AMPPNP (PDB code 1ATP, 1CDK) in the presence of pseudosubstrate, "closed" or "intermediate" for various inhibitors, to "open" for unliganded PKA (PDB code 1J3H; Akamine et al., 2003). The extent of openness can be quantitatively characterized by using several parameters. One is the occurrence of a hydrogen bonding distance between NE2 of His87 from helix C and pThr197 (O3P) of the activation loop in the closed conformation. By this measure, the structures of PKA-Y and PKA-1152 (Figure 3, green ribbon, 2.5 Å; yellow ribbon, 2.6 Å) represent closed lobe structures, whereas the PKA-1077 structure is—with a 4.6 Å separation—an open structure (Figure 3, red ribbon).

Glycine Loop

The flexibility of the glycine loop is demonstrated by relatively high B factors and by the occurrence of dif-

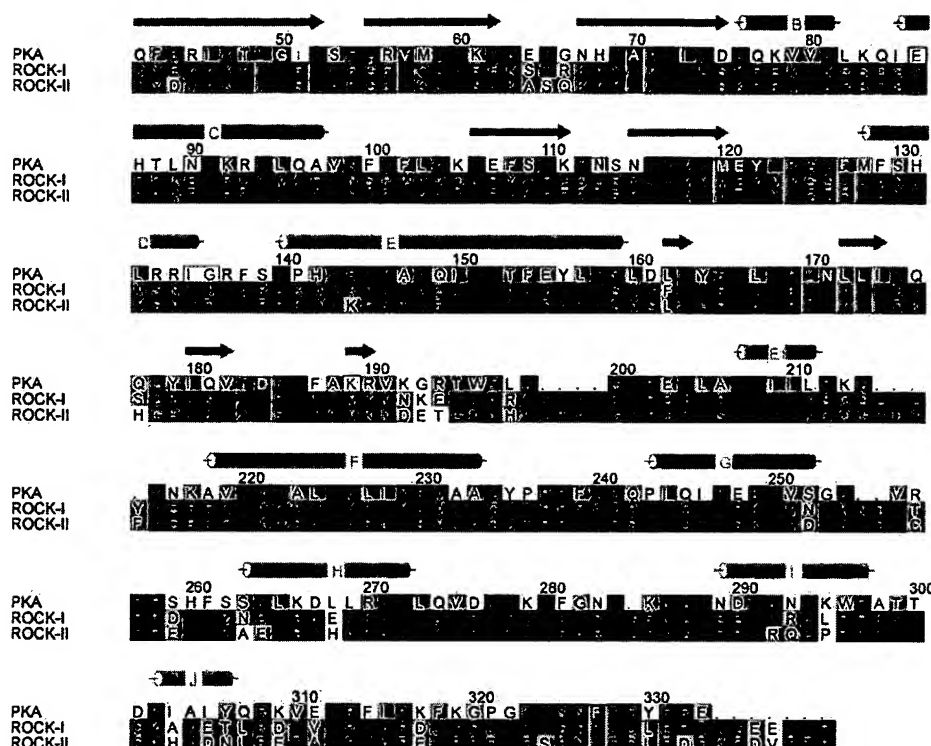


Figure 2. Sequence Alignment of PKA and the Highly Similar Rho Kinase Family Members ROCK-I and ROCK-II

Blue backgrounds indicate identical residues whereas brown indicates conservative exchanges. Secondary structure elements of PKA (from Bossemeyer et al., 1993) are indicated above the PKA numbering. The most highly conserved kinase residues are shown in red letters. Inhibitor contacts are marked with light violet letters and boxes. Additionally, contacts with H-1152P in the second binding site are indicated in green.

ferent positions in all three structures. The differing positions create ATP ligand binding sites that are progressively more open among structures 1CDK (PKA/

PKI(5-24)/MnAMP-PNP) (Bossemeyer et al., 1993), PKA-Y, PKA-1152, and PKA-1077 (3, 4) (Figure 3C, blue, green, yellow, and red ribbon, respectively). There is also evi-

Table 1. Data Collection and Refinement Statistics

	Y-27632	H-1152P	HA-1077
Data Collection			
Space group	P2 ₁ 2 ₁ 2 ₁	P2 ₁ 2 ₁ 2 ₁	P2 ₁ 2 ₁ 2 ₁
Cell (a, b, c) (Å)	74.0, 76.6, 80.7	74.2, 76.4, 81.8	70.3, 73.7, 79.1
Resolution range (Å)	15.8–2.0	10.91–1.9	20–2.2
Completeness (%) [last shell]	97.8 [88.7]	91.8 [56.0]	82.4 [59]
I/σ(I) [last shell]	4.2 [1.4]	7.5 [0.6]	7.5 [1.3]
R _{sym} [last shell]	0.12 [0.50]	0.06 [0.51]	0.10 [0.34]
Refinement			
Number of atoms used in refinement	3104	3245	2914
R factor (%)	18.1	17.9	21.7
Free R factor (%)	22.9	21.7	29.3
Free R value test size (%)	10.1	5.0	5.0
Reflections used	27,774	32,327	16,761
Standard Deviation from Ideal Values			
Bond length (Å)	0.016	0.017	0.021
Bond angles (°)	1.440	1.491	1.83
Temperature Factors			
All atoms	39.4	25.1	24.4
Main chain/side chain atoms PKA	37.6/40.0	22.9/25.5	23.1/25.2
Main chain/side chain atoms PKI	32.8/36.7	21.0/23.9	26.6/29.8
Inhibitor atoms	38.3	33.3	23.2
Solvent molecules	50.3	36.6	25.8
Inhibitor atoms (second)		21.2	
Detergent		43.3	

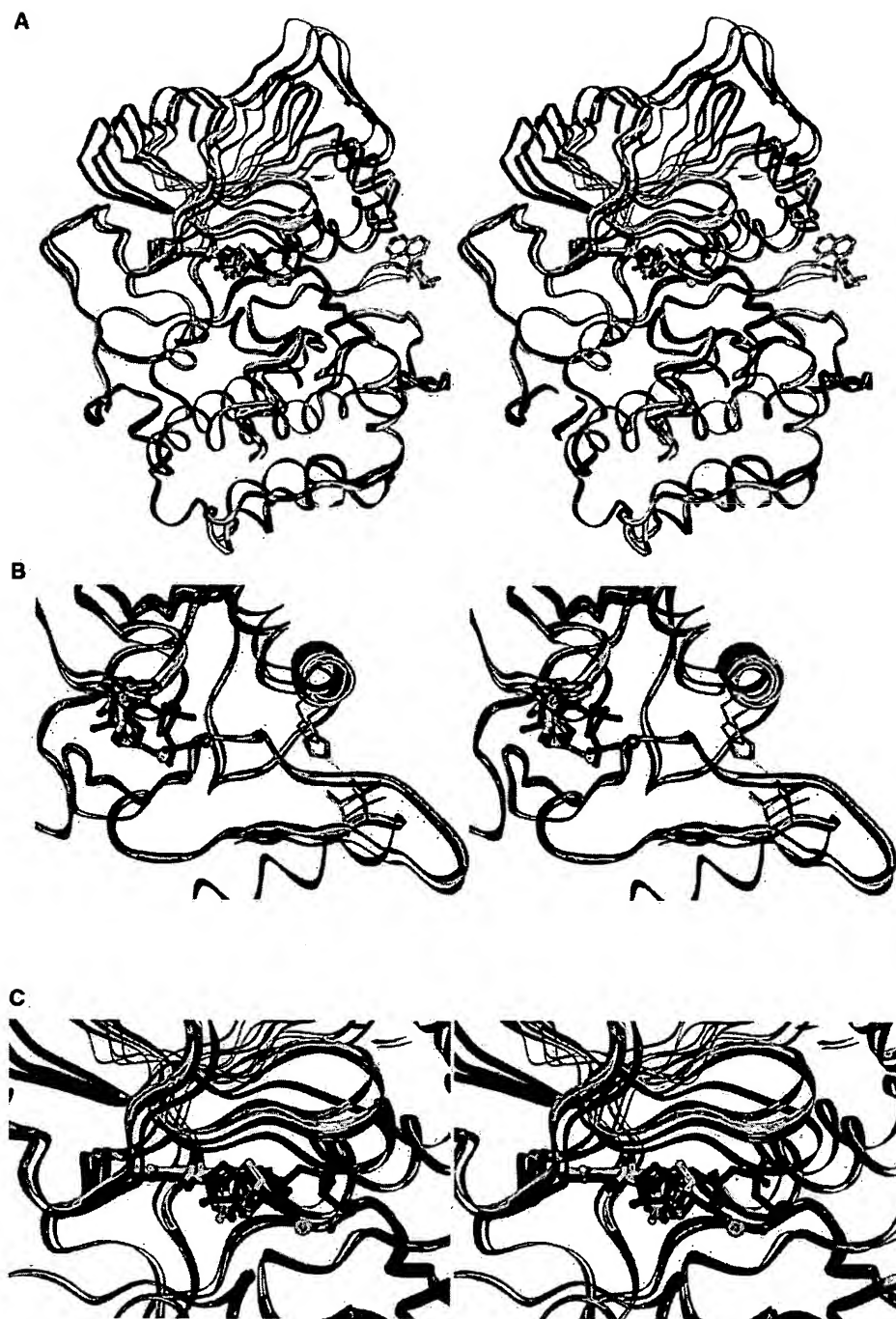


Figure 3. Binding of the Inhibitors to PKA

(A) Open-closed conformations illustrated by an overlay of all three inhibitor structures (Y-27632, green; HA-1077, red; H-1152P, yellow) and the PKA-AMP-PNP (1CDK) complex (blue) for comparison.

(B) In the PKA-HA1077 structure, helix C is further away from the activation loop, and the salt bridge His87-pThr197 is not formed.

(C) A closer view of the binding pocket shows the inhibitor binding modes relative to AMP-PNP and the positions of the flexible glycine-loop. The inhibitor molecules occupy both the adenine and the ribose pocket, but not the triphosphate binding site.

dence for multiple conformations of the glycine flap within a single crystal (data not shown). PKA-Y electron density maps suggest the partial occupancy of a more closed position of the glycine flap (especially involving

turn residues Ser53-Phe54-Gly55), similar to that previously observed with the H7 and H8 inhibitor complex structures of PKA (Engh et al., 1996). Because none of the cocrystallized inhibitors occupies this site, they do

not have the structuring effect of the triphosphoryl group of ATP with its contacts to the glycine loop.

Inhibitor Binding

The chemical structures of the three inhibitors are shown in Figure 1. They originate from two different chemical classes but share the general architecture of a planar ring system linked to a saturated ring. In the case of Y-27632, a pyridine ring is connected by an amide to a saturated para-aminoethyl cyclohexane ring. HA-1077 and its derivative H-1152P share the basic scaffold of an isoquinoline ring connected to a homopiperazine ring by a sulfonamide linker. Compared to HA-1077, H-1152P has two additional methyl groups, one at the isoquinoline ring and another at the homopiperazine ring. These two methyl groups are thus responsible for the unique binding properties of the derivative. The planar ring systems occupy the adenine subsite, while the linker and the saturated rings occupy the ribosyl subsite. The triphosphate subsite is not used by any of the inhibitors (Figures 3C and 4).

Figure 4 shows the inhibitors in the ATP pocket and the $F_o - F_c$ electron density maps with the inhibitor atoms omitted contoured at 2.5σ . Y-27632 is well defined in the electron density (Figure 4A), which, however, does not uniquely identify the orientation of the cyclohexane ring chair conformer (see next paragraph). The typical intrinsic flexibility of the seven-membered homopiperazine rings of HA-1077 and H-1152P is reflected in less well defined electron densities in this region (Figures 4B and 4C). The electron density of H-1152P (Figure 4C) has gaps in portions of the homopiperazine ring too, contradicting expectations that the two extra methyl groups should stabilize the ring conformations relative to HA-1077. In contrast, the homopiperazine ring of the H-1152P inhibitor bound outside the catalytic cleft close to Thr197 of the activation loop binds with a clearly defined electron density for the whole inhibitor (Figure 4D).

Binding of Y-27632

With a K_D value of $17.5 \pm 3.87 \mu\text{M}$ by surface plasmon resonance spectroscopy (SPR) and a $25 \mu\text{M}$ K_i value from previous kinetic data (Uehata et al., 1997), Y-27632 has the weakest PKA inhibition of the compounds studied here (Table 2). For Rho-kinase, however, Y-27632 has a K_i value of 140 nM . This pronounced selectivity for Rho-kinase is further emphasized by data showing that Y-27632 inhibited only one other protein kinase (PRK2) from a panel of 34 kinases with similar potency (Davies et al., 2000).

Despite the relatively weak PKA inhibition, Y-27632 cocrystallized readily and is clearly localized in the electron density, although two orientations of a chair conformer of the cyclohexane ring are possible (Figure 4A). To analyze the binding of Y-27632 to PKA, we considered binding surfaces and hydrophobic (van der Waals), and hydrophilic (H bonds) interactions for both conformations (see Tables 3–5). The buried surface areas (188 or 189 \AA^2) and numbers of van der Waals contacts (64 or 67) are similar for the two conformations. The van der Waals contacts are formed to residues from the ATP

binding pocket, especially to the invariable Val57 with 9 or 10 side chain contacts and to the more variable Val123 with 12 contacts. Four contacts are formed to Phe327, the residue characteristic of the AGC kinases that is inserted into the ATP pocket from the C-terminal strand of the kinase. The two conformations differ most at the terminal aminoethyl group, which adopts either one H bond between N17 and the backbone carbonyl oxygen of Thr51 (2.83 \AA) (Table 4; Figure 5A), or a H bond with Asn171 (OD1) (2.89 \AA) and Asp184 (OD1) (2.93 \AA) (Table 4). The pyridine ring in both conformations forms a H bond between pyridine nitrogen atom N1 and backbone nitrogen of Val123 (2.93 \AA) (Figure 5A), the hydrogen bond donor at the hinge region between the N- and C lobes that binds to nearly all known ATP-site inhibitors (Engh and Bossemeyer, 2001). Y-27632 also binds via water molecules sandwiched between N7 and the carboxylate of Glu127 and the backbone carbonyl of Leu49.

HA-1077

As described in the introduction, HA-1077, also known as fasudil, is used to treat cerebral vasospasm and works via Rho-kinase inhibition. However, it also inhibits several other kinases in the μM range (Davies et al., 2000). Our SPR data show a K_D value of $5.7 \mu\text{M}$ for PKA; published data include a K_i value of $1.0 \mu\text{M}$ (Ikenoya et al., 2002) (Table 2). HA-1077 makes three H bonds to PKA (Figure 5B; Table 4). Like other isoquinoline inhibitors (Engh et al., 1996), one H bond is formed between the isoquinoline N (N15) to the backbone N of Val123 (2.8 \AA). The homopiperazine amine (N4) forms H bonds with the backbone carbonyl oxygen of Glu170 (3.25 \AA) and the side chain of Glu127 (OE2) (2.69 \AA), the latter at the position of the ribose 3'OH group in the ATP-PKA complex (Bossemeyer et al., 1993). A Glu127-inhibitor contact was observed for staurosporine (Prade et al., 1997), but not with the other isoquinoline sulfonamide inhibitors (Engh et al., 1996). A total of 81 van der Waals contacts are formed to the residues of the ATP pocket. Most contacts are to Val123 (13), Val57 (11), and Thr183 (11) (Table 4).

H-1152P

H-1152P is a derivative of HA-1077 with enhanced specificity for Rho-kinase (Sasaki et al., 2002). For PKA, it has a K_D (SPR) or K_i (Ikenoya et al., 2002) value of 1.06 or $0.63 \mu\text{M}$, respectively (Table 2). With a K_i of 1.6 nM , H-1152P inhibits Rho-kinase potently (Sasaki et al., 2002; Ikenoya et al., 2002). The H-1152P molecule that binds to the ATP pocket makes only one H bond contact (from the isoquinoline N [N16] to the backbone NH of Val123 [3.0 \AA]) (Figure 5C; Table 3). As with the other inhibitors described here, Val57 and Val123 are involved in many van der Waals contacts; in contrast to the other two inhibitors, Leu173 and Leu49 additionally form many contacts (Leu173: 12 with H-1152P versus 2 with HA-1077; and Leu49: 8 with H-1152P versus 2 with Y-27632 and 4 with HA-1077).

In its second binding site close to helix C and the activation segment, H-1152P makes five H bond contacts, three to the Thr197-phosphoryl group in the acti-

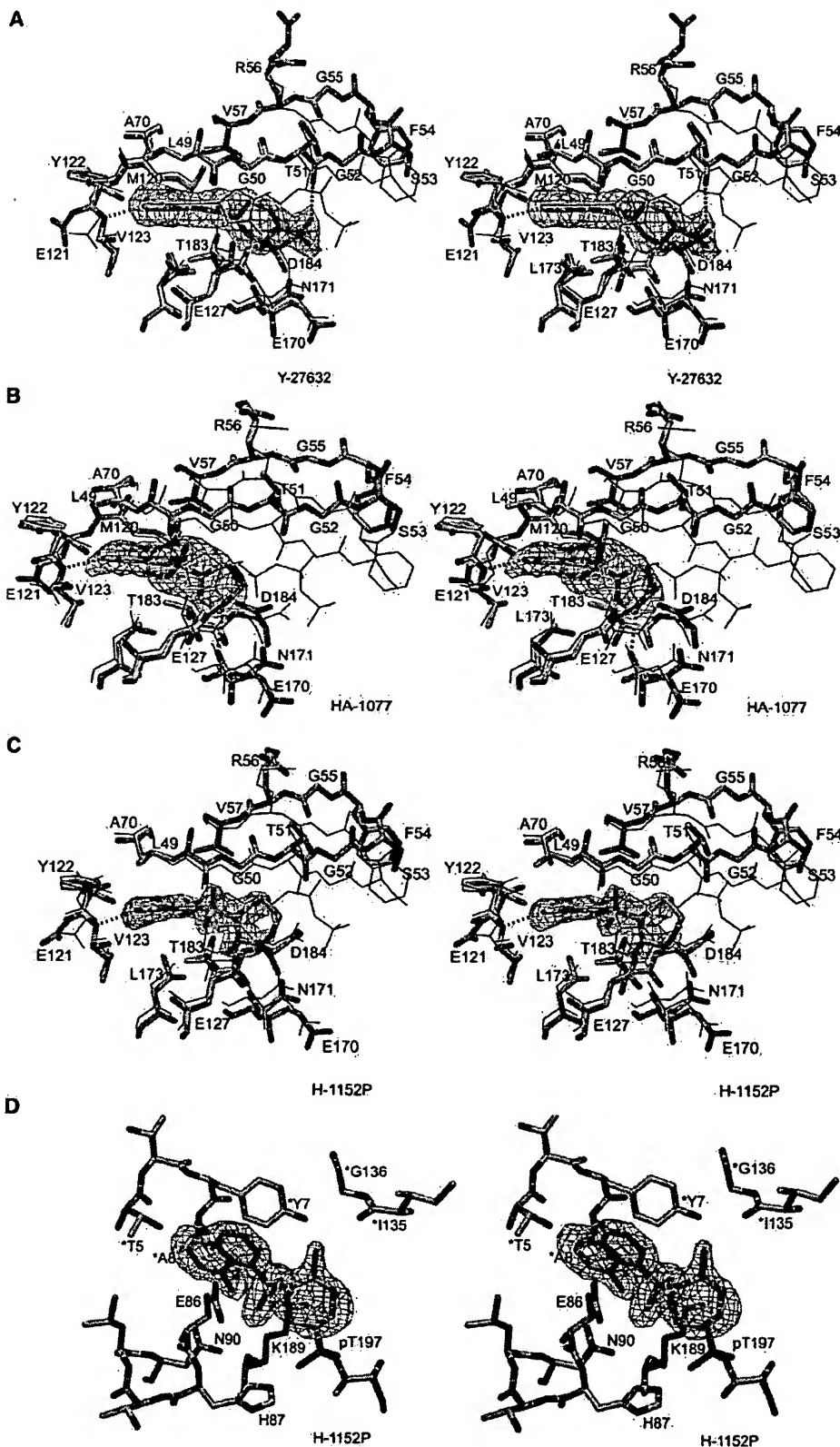


Figure 4. Structure of Inhibitor Binding Sites with Electron Density Maps

Shown are the three PKA bound inhibitors with corresponding $F_o - F_c$ electron density maps (inhibitor atoms omitted) contoured at 2.5σ . Amino acid residues in the vicinity of the inhibitors are shown. H bonds between inhibitor atoms and enzyme residues are depicted as dotted lines. The PKA-PKI-AMP-PNP complex is drawn as fine black lines. Inhibitors (A) Y-27632, (B) HA-1077, and (C) H-1152P bind in the ATP pocket. (D) The second H-1152P molecule, which occupies a binding site at the enzyme surface in contact with the activation loop and helix C, is well ordered, indicated by its well defined electron density. (Residues from a symmetry-related molecule are colored yellow.)

Table 2. Inhibitor Binding Properties

Inhibitor	Y-27632	HA-1077	H-1152P
K _D PKA	17.5 ± 3.9 μM	5.7 ± 1.2 μM	1.1 ± 0.1 μM
K _i PKA*	25 μM	1.0 μM	0.63 μM
K _i RHO*	0.14 μM	0.33 μM	0.0016 μM
Buried surface	188(189)	196.4	215.7
VDW contacts	64(67)	81	96
H bonds	2(3)	3	1

K_D values from surface plasmon resonance spectroscopy (SPR) analysis, Chi² smaller than five, two independent experiments, Inhibition constants correlate well with the buried surface and number of van der Waals (VDW) contacts but not with number of H bonds.

*K_i values from literature (Ikenoya et al., 2002; Sasaki et al., 2002).

vation loop, one to Lys189 also of the activation loop, and one to Thr5 of PKI(5-24) from a symmetry-related molecule (Figure 5D). The inhibitor is embedded in a network of water molecules, thus making additional contacts via water to Asn90 from helix C and Thr195 from the activation loop. In this activation loop binding site, the inhibitor electron density is well connected and verifies a unique conformation of the homopiperazine ring with no apparent disorder (Figure 4D). Significant van der Waals contacts are made to the side chain of Glu86 from helix C, which changes its side chain conformation (compared to 1CDK) to accommodate the inhibitor. Further binding studies are necessary to determine the relevance of the second binding site in solution.

Binding Specificities of Y-27632, HA-1077, and H-1152P

Comparison with the Mn²⁺-AMP-PNP complex identifies only small induced-fit movements of ATP pocket residues associated with binding of the three inhibitors. The side chain of Asp184, which chelates a metal ion in the active complex, is oriented toward the opening of the active side cleft in the AMP-PNP complex and in the PKA-Y or PKA-1152 structure. In the PKA-1077 structure, however, Asp184 adopts a different rotamer (Figure 5B), which points toward the homopiperazine

ring, increasing van der Waals contacts and apparently enhancing hydrophobic effect binding. A similar reorientation of this side chain was observed in the H8-inhibitor complex of PKA (Engh et al., 1996), where Asp184 makes an H bond contact to the amide of the inhibitor side chain. Thr183 and Leu173 in the PKA-Y structure apparently have two conformations that were each modeled with an occupancy of 0.50 (data not shown). These two amino acid residues interact with each other by van der Waals contacts which limit their degree of conformational freedom, indicating mutually dependent rotamer conformations and a concerted induced fit movement.

The three inhibitors bind with moderate binding strengths to PKA. Their differing affinities (Table 2) correlate with the different numbers of van der Waals contacts and with the contact surface area between the inhibitors and enzyme residues (buried surface) (Table 2). H-1152P, which has the highest affinity for PKA, also has the highest number of van der Waals contacts and the largest buried surface (215.7 Å²). Y-27632, with the weakest PKA binding, has the smallest total number of van der Waals contacts and a buried surface area of 189.9 Å². A relationship of buried surface areas and affinities of PKA inhibitors has been noted previously (Engh and Bossemeyer, 2002). The simplest measure of hydrophilic binding interactions—the number of inhibitor-protein H bonds—does not correlate with PKA binding affinities. This is typical of enzyme inhibitors and reflects the existence of competing hydrophilic interactions in inhibitor solvation. H-1152P possesses only a single H bond from its isoquinoline ring to Val123 in the hinge region. This H bond to Val123 or its equivalent is nearly universal among protein kinase-inhibitor complexes and exists in all PKA-inhibitor complexes crystallized so far (Narayana et al., 1999; Prade et al., 1997; Engh et al., 1996). Indeed, a survey of ligand binding properties from protein kinase crystal structures in the protein data bank identifies only two inhibitors that lack such an interaction, namely CK2/Emodin (1F0Q) (Battistutta et al., 2000) and p38/BPU (1KV1). All other ligands make one, two, or three H bonds to the hinge polypeptide, i.e., always one to the hinge region backbone amide of the Val123

Table 3. Van der Waals Contacts of the Inhibitors to PKA Enzyme Residues

Residue	Y Chair1	Y Chair2	HA-1077	H-1152P	Interaction via
L49	2	2	4(1p*)	8(1p*)	main chain/side chain
G50	—	1	2	4(1p*)	main chain
T51	3	3	—	5	main chain
V57	9	10	11	12	side chain
A70	4	4	6	7	side chain
M120	1	1	4	4	side chain
E121	2(1p*)	2(1p*)	3(1p*)	3(1p*)	main chain
Y122	6	6	7	6	main chain/side chain
V123	12	12	13	10(1p*)	main chain/side chain
E127	—	—	4	4(2p*)	side chain
E170	2	2	2	4	main chain
N171	6	4	2	2	main chain/side chain
L173	5	6	2	12	side chain
T183	4(1p*)	6(1p*)	11	7	side chain
D184	4	4	4	—	side chain
F327	4	4	6	8	side chain
Total	64(2p*)	67(2p*)	81(2p*)	96(6p*)	

Residues that have side chain contacts with the ATP-site ligands and differ between Rho-kinase and PKA are in bold.

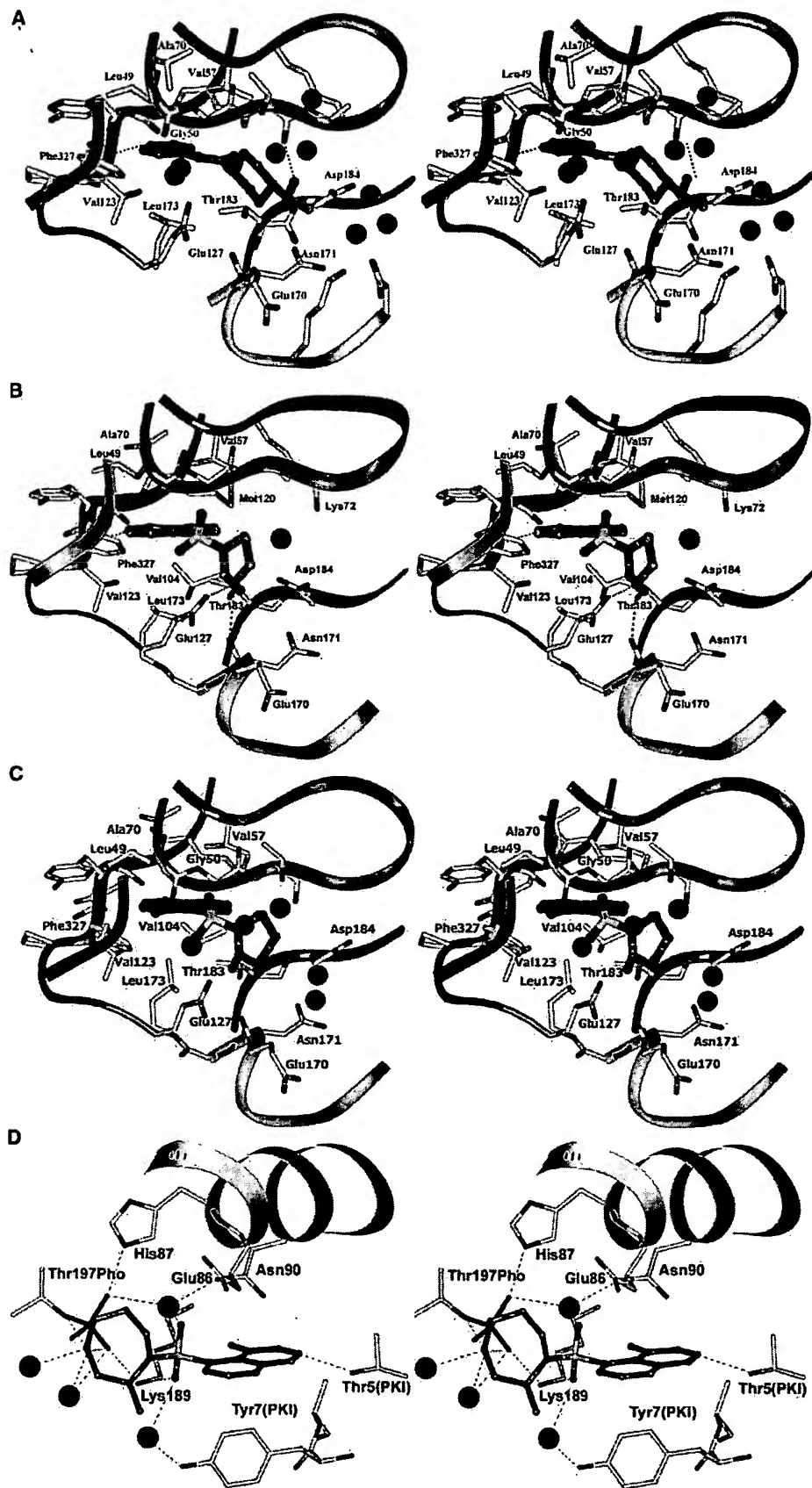


Figure 5. Inhibitor Binding Modes

Binding of Y-27632 (A) and HA-1077 (B) to PKA to the ATP binding site. H-1152P binds in two positions: (C) in the ATP binding site and (D) in a second binding site at the surface interacting with the activation loop and helix C in a crystal contact region.

Table 4. H Bonds between Inhibitor Atoms and PKA Enzyme Residues

H Bonds	Inhibitor Atom	PKA Residue and Atom	Distance (Å)	Interaction via
Y-27632 chair 1	N1	Val123(N)	2.9	main chain
	N17	Thr51(O)	2.8	side chain
Y-27632 chair 2	N1	Val123(N)	2.9	main chain
	N17	Glu171(OD1)	2.9	side chain
	N17	Asp184(OD1)	2.9	side chain
HA-1077	N15	Val123(N)	2.8	main chain
	N4	Glu170(O)	3.3	main chain
	N4	Glu127(OE2)	2.7	side chain
H-1152P	N16	Val123(N)	3.0	main chain

H bonds between inhibitor and PKA atoms are listed together with the distance (in Å) and information about main chain or side chain interaction.

homolog, and, in addition, further contacts to the homologs of the Val123 and/or Glu121 carbonyl atom(s). This interaction is conserved despite the wide chemical diversity of small molecule protein kinase inhibitors. Thus the interaction is critical for good inhibitors, or conversely stated, the kinase is apparently unable to compensate for the desolvation of the Val123NH equivalent group if a potential inhibitor lacks the appropriate hydrogen bond acceptor. Hydrogen bonds from other residues that bind to the adenosine group of ATP appear to be of less importance for protein kinase inhibitor binding. Two H bonds that are formed between the ribosyl hydroxyl groups of AMP-PNP and the Glu127 carboxyl and the Glu170 main chain carbonyl groups have counterparts in the PKA-1077 structure. The presumably doubly protonated secondary amine (N4) of HA-1077 forms hydrogen bonds both to the carboxyl group of Glu127 and to the backbone carbonyl of Glu170. In the case of H-1152P, these contacts are not formed, because contacts between Thr183 and Leu173 of the enzyme and homopiperazine methyl group (C10) of the inhibitor apparently shift the heptamer ring by ca. 1.5 Å in comparison to HA-1077. Consequently, the distances to E170(O) (4.2 Å) and E127 (OD1) (3.57 Å) are too large for tight H bonds. The overlay of the two structures in Figure 6 shows the colocalization of the isoquinoline atoms with respect to the surrounding residues, and the divergent positions of the homopiperazine rings. Although H-1152P makes only one hydrogen bond to the enzyme, the two extra methyl groups increase the number of van der Waals interactions (Table 3) and enlarge the buried surface area, which probably leads to the enhanced affinity of H-1152 in comparison to HA-1077.

The Second Binding Site of H-1152P

The second molecule of H-1152P in PKA-1152P is found in contact with the activation segment and helix C, the two structural elements critical for protein kinase inactivation (Engl and Bossemeyer, 2001), which suggests a potential for activity modulation. Because the residues in contact with this second inhibitor molecule are not conserved between PKA and Rho-kinase, the observed second H-1152P binding site likely appears to be unique for PKA. Further, this site is an important contact region for protein-protein interaction with the regulatory subunits of PKA (Orellana et al., 1993; Gibbs et al., 1992). Occupation of this site with a small molecule derivative could provide a means to abolish negative regulation of PKA by the R subunits. If this site could be explored

more generally as a docking site for small molecules in drug design, other important interactions, for example cyclin binding to cyclin-dependent kinases, could be targeted as well.

Comparison of the Rho-Kinase and PKA

Ligand Binding Sites

Although the three inhibitors bind and inhibit PKA, all of them bind Rho-kinase more tightly than PKA. Because of the high conservation of the protein kinase fold, especially for closely related kinases, one can assume that the side chains that are nearest to the inhibitor are the major determinants of selectivity. The sequence alignment of the kinase domains of Rho-kinase and PKA (Figure 2) show either conservation (blue coloring) or conservative exchanges (beige coloring) over large parts of the kinase domain. Rho-kinase has several exchanges relative to PKA, but only four of them make side chain interactions with the inhibitors: Thr183Ala, Leu49Ile, Val123Met, and Glu127Asp. These exchanges very likely are responsible for the effects of the extra methyl groups of H-1152P compared to HA-1077 on specificity toward Rho-kinase. The two methyl groups lead to a 200-fold higher affinity for Rho-kinase (Table 2), but only a 2- to 5-fold higher affinity for PKA, or in other words, cause a 40- to 100-fold increase in selectivity.

The residues nearest to the H-1152P methyl groups are Leu49, Leu173, Thr183, and Phe 327, thus involving directly two of these four PKA to Rho-kinase exchanges, and one residue (Phe 327) specific for most AGC kinases. The Thr183Ala substitution would provide more room for the C10 methyl group and possibly allow more rotamer conformations of Leu173. The interactions of C10 with Thr183 and Leu173 in PKA appear to force the H-1152P homopiperazine away from its position in the PKA-1077 structure (Figure 6), presumably at some energy cost. The exchange of Thr183Ala in Rho-kinase would, however, allow the homopiperazine to retain its preferred binding orientation. Consequently, H-1152P might be able to form hydrogen bonds to both the Glu170 homolog and to the aspartyl residue occupying the Glu127 homologous position in Rho-kinase. Although the side chain of the aspartyl is shorter by one methylene group, this should not affect its ability to hydrogen bond a homopiperazine nitrogen in a position similar to that of HA-1077 in PKA.

The effect of the Leu49Ile exchange is more difficult to evaluate because of the number of possible rotamer

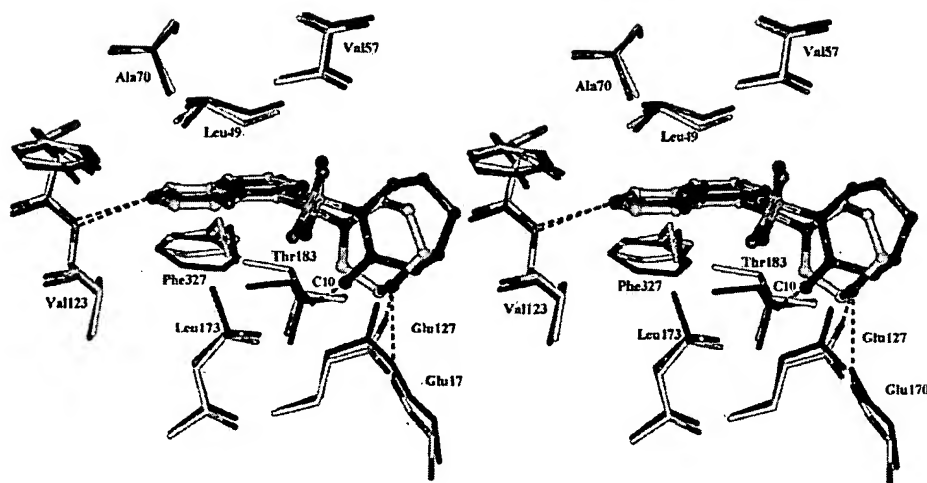


Figure 6. Comparison of HA-1077 and H-1152P

Overlay of HA-1077 and H-1152P demonstrates the colocalization of the isoquinoline atoms with respect to the surrounding residues. Both inhibitor molecules form an H bond to the backbone amide of Val123 in the hinge region. The position of the homopiperazine rings, however, diverge by ca. 1.5 Å. Consequently, H bonds between the homopiperazine nitrogen and Glu127 and Glu170 are formed only in the PKA-1077 complex. The contact between C10 and Thr183, which prevents as a steric clash a HA-1077-like positioning of the H-1152P homopiperazine ring, is shown as a red double arrow.

conformations of the isoleucine residue. Most rotamers of an isoleucine modeled into the Leu49 position increase the number of interactions with the inhibitor or cause steric clashes with the inhibitor isoquinoline sulfonamide moiety. Because of the branching of the isoleucine side chain at the C β , in contrast to a leucine residue, the inhibitor binding pocket is narrowed in the expected binding region of the isoquinoline methyl and sulfonamide groups, also close to the Phe327 homolog; this appears to favor H-1152P binding. It is likely that the isoquinoline methyl group of H-1152P then additionally contributes to a productive interaction by a mutual increase in the number of van der Waals interactions with the isoleucine side chain.

How or even whether the Val123Met exchange might affect binding selectivity is unclear. A relatively large number of van der Waals contacts (Table 3) are formed to all three inhibitors. A methionine residue is found at this position in several kinases with known structures, including Erk, p38, Src, and Abl. In all these cases, the methionine side chain is oriented away from the adenosine subsite, providing little contact beyond the C γ atom. By analogy, this methionine side chain therefore is not likely to be a major factor in H-1152P specificity for Rho-kinase. In addition, a large number of van der Waals contacts are found with the residue Phe327, which is conserved in most members of the AGC group of protein kinases. Phe327 makes attractive additional interactions with the isoquinoline extra methyl group of H-1152P in PKA, compared to HA-1077.

Taken together, the higher affinities of HA-1077 and H-1152P for Rho-kinase—and the especially strong binding of the H-1152P derivative to Rho-kinase—can be explained largely by three factors: the Thr183Ala exchange and the concomitant relaxation of the steric clash between the inhibitor C10 methyl group and Thr183 and Leu173 (Figure 6). This in turn allows the

inhibitor to bind with the optimal geometry and hydrogen bonding pattern as observed for HA-1077 in PKA. Further, the exchange Leu49Ile presumably optimizes the van der Waals interactions—i.e., inhibitor fit—because of the position of the branch in the side chain. Whether additional effects arise from the Val123Met exchange remains to be seen. Last but not least, the AGC-kinase typical Phe327 residue makes attractive contacts with all inhibitors, but especially with the C22 extra methyl group of H-1152P.

The higher affinity of Y-27632 for Rho-kinase is more difficult to rationalize based on sequence considerations. One determinant is probably the Leu49Ile exchange. The shorter branched methyl group is likely to provide additional van der Waals interactions with three different parts of the inhibitor molecule, thereby increasing the overall binding surface area and improving the quality of the fit. The absence of steric clashes in the region of Thr183 (and Glu127), however, obscures analysis of possible contributions of the corresponding exchanges at these positions to the higher affinity of Y-27632 in Rho-kinase. Regarding the Val123Met exchange, the likelihood that it is oriented away from the inhibitor as discussed above leads to the conclusion that Rho-specific interactions with the Met side chain are possible but unlikely. A similar compound, Y-30141, which differs from Y-27632 by a pyrrolopyridine ring replacing the pyridine ring, has a similar inhibitory profile, but a 10-fold higher affinity for Rho-kinases (Ishizaki et al., 2000). Its selectivity, i.e., the ratios of the IC₅₀ for Rho-kinase to that for other kinases, however, is about 10-fold lower. In the binding pocket, the extra pyrrolidine group is likely to make one additional hinge region contact with its proton donor in the five ring, either to the carbonyl of Glu121 (PKA numbering) or, if rotated 80°, to the carbonyl of Val123. The higher affinity can also be explained by the larger surface of the planar double

Table 5. Conservation of Residues in the Binding Pocket that Differ between PKA and Rho-Kinase

Residue in PKA	PKA	No.*	%	Rho kinase	No.*	%	Contact
49	Leu	241	49.1	Ile	186	37.9	side chain/backbone
51	Thr	18	3.7	Arg	71	14.5	backbone only
123	Val	76	15.5	Met	123	25.1	side chain/backbone
127	Glu	76	15.5	Asp	158	32.2	side chain
170	Glu	140	28.5	Asp	59	12.0	backbone only
183	Thr	76	15.5	Ala	142	28.9	side chain

Shown are residues in contact with the inhibitors that differ between PKA and Rho-kinase according to the alignment from www.kinase.com (Manning et al., 2002). The total number of kinases in the alignment is 491. The number (No.*) as well as percentage (%) of kinases with the same corresponding residue (numbering according to PKA) to PKA and Rho-kinase, respectively, were calculated. Contacts to the inhibitor via main chain or side chain are indicated. Residues that have side chain contacts with the ATP-site ligands are in bold.

ring compared to the single ring of Y-27632. These additional interactions can be assumed to increase the binding potency. The drop in selectivity can be explained if one assumes that the interactions which determine the selectivity for these Y-class inhibitors remain the same for both inhibitors and thus are less relevant in the case of the better binding Y-30141.

Selectivity of the Inhibitors for Rho-Kinase Relative to Other Kinases

We have argued above that many of the interactions with residues which differ between Rho-kinase and PKA explain why HA-1077, H-1152P, and Y-27632 bind more tightly to Rho-kinase than to PKA. The amino acid residues in question are, however, common in the kinase family. From the available kinetic data, at least HA-1077 and Y-27632 show selectivity for only a few kinases (less data is available for H-1152P). The question arises whether selectivity arises from a unique combination of specific amino acid residues or simply from the sum of a small number of individual interactions that can be considered independently of one another.

Using a sequence alignment of 491 human kinases (see e.g., www.kinase.com; Manning et al., 2002), we built a database to calculate the frequency of certain amino acid residues and of their combinations. Table 5 shows the degree of conservation for the residues that are different between PKA and Rho-kinase. Either isoleucine and leucine is found at the Leu49 position in most kinases, with leucine more frequent than isoleucine. Also, an alanine in the Thr183 position (28.9%) is common (and more common than threonine with 15.5%). Relatively high frequencies are found also for Rho-kinase side chains of methionine in the Val123 position (25.1%) and aspartic acid at the Glu127 position (32.2%). While these residues are common when considered individually, the combination of all four is nearly unique. Only 6 out of 491 kinases possess the same combination, 3 from the subgroup of cell cycle related kinases (CRK7, CCRK, and CHED), and 3 tyrosine kinases, MUSK, MET and RON.

If we consider additionally the AGC characteristic residue Phe327, the combination of inhibitor binding side chains seen in Rho-kinase becomes truly unique. Phe327, located on a C-terminal strand that stretches across the catalytic cleft, interacts with its aromatic side chain with the adenosine moiety of ATP, as well as with

all kinase inhibitors cocrystallized with PKA so far. The three inhibitors in this study make four (Y-27632), six (HA-1077), or eight (H-1152P) van der Waals contacts to Phe327. Sequence alignments of PKA versus ROCK-I or ROCK-II indicate that Rho-kinase also has a phenylalanine residue in a position homologous to Phe327 (Figure 2). The crystal structure of AGC kinase PKB shows residue Phe439 in a position identical to Phe327 in PKA (Yang et al., 2002). More distantly related kinases, however, do not have a corresponding C-terminal strand with a recognizably equivalent aromatic side chain (although other strands, domains, or subunits may contribute a similar chain). Thus, the combination of all five residues, Ile (Leu49), Ala (Thr183), Asp (Glu127), Met (Val123), and Phe (Phe327), is an exclusive feature of Rho-kinase. It should be noted that these residues are also among the ones with the largest numbers of contacts to the inhibitors, especially to H-1152P (Table 3). And, while the individual residues exchanges may be relatively conserved, in combination they generate a uniquely shaped inhibitor binding pocket with unique electronic properties, rationalizing the selectivity of Rho-kinase for certain protein kinase inhibitors, such as HA-1077, H-1152P, and Y-27632.

Conclusions

The one common feature of all protein kinases is ATP binding at a highly conserved ATP binding site with highly conserved binding interactions. The highest degree of conservation is seen with the catalytic residues that are absolutely conserved across the entire protein kinase family. The tertiary structure that forms the ATP binding site is apparently highly conserved in the active state of the protein, but this conclusion depends upon extrapolation from the still relatively few active structures that have been solved. The primary sequences are mostly highly conserved at the residues that form the triphosphoryl binding site, presumably because this represents the catalytic site. Conserved features of the adenosine binding site are restricted to the backbone contacts of the hinge region and to a generally hydrophobic or aromatic environment surrounding adenine; residues at positions homologous to Val57 and Ala70 in PKA are additionally conserved as small hydrophobic residues. Otherwise, there is considerable variability in sequence and, when considering inactive forms, in structure among protein kinases. Physiological

roles for this variability are generally recognized only for those cases where specific events such as phosphorylation are seen to modulate activity. Most protein kinases bind ATP with low micromolar binding constants, consistent with the need for exchange of ATP, ADP, and unbound states. Thus, sequence and structural variability at the ATP binding pocket has few known physiological roles regarding ATP binding, but is crucial for the selectivity of nonphysiological, high affinity ATP-site ligands, such as low molecular weight protein kinase inhibitors.

Crystallographic studies of enzyme-inhibitor complex structures provide information directly relevant to the drug design tasks of optimizing potency and selectivity. For protein kinases, these tasks are complicated by several factors. First, the substrate binding sites are relatively flexible, so that individual structures do not fully characterize an enzyme. Secondly, as discussed above, the natural substrates generally bind weakly, so that tight binding inhibitors are not obviously derivable from substrates. Third, the similarity of the ATP binding sites of active protein kinases means that inhibitors are likely to bind many of the ca. 600 kinases other than the target kinase.

The development of potent and selective kinase inhibitors and their success as therapeutics has demonstrated that problems anticipated with protein kinases as targets can be overcome. The process of optimization of such inhibitors can be improved. Of the inhibitors described here, only H-1152P was specifically designed to target Rho-kinase. The crystal structures, however, show how they bind and identify the probable determinants of Rho-kinase selectivity. This information focuses strategies for chemical synthesis and should improve the overall efficiency in achieving desired inhibition profiles. Cocrystal structures of Rho-kinase with inhibitors are needed to verify and possibly refine the model. Verification of the model would also verify the approach of using PKA as a surrogate for Rho-kinase crystallization, which might remain a preferable approach if Rho-kinase crystallization proves difficult, or if only inactive conformations of Rho-kinase will be crystallizable.

Experimental Procedures

Protein Expression and Purification

Recombinant bovine $C\alpha$ catalytic subunit of cAMP-dependent protein kinase (which differs from the human protein at two positions: Asn32Ser and Met63Lys) was soluble expressed in *E. coli* BL21(DE3) cells and then purified via affinity chromatography and ion exchange chromatography as previously described (Engh et al., 1996). Three-fold phosphorylated protein was used for crystallization of Y-27632 and H-1152P, whereas 4-fold phosphorylated protein successfully formed cocrystals with HA-1077.

Crystallization

Y-27632 and HA-1077 were purchased from Calbiochem. Y-27632, HA-1077, and H-1152P were cocrystallized with PKA and PKI(5-24) at 75 mM LiCl, 25 mM MesBisTris (pH 6.4). Hanging drop vapor diffusion against 15% methanol as precipitant was used to obtain ca. $100 \times 100 \times 500 \mu\text{m}$ crystals.

Biacore Sensor Chip Preparation

Proteins used for Biacore analysis were dialyzed two times with the 400-fold volume of 50 mM MOPS (pH 6.8), 10 mM MgCl_2 , and 50 mM KCl (Gassel et al., 2003). Coupling of PKA to a CM5 Biosensor

chip via amine group linkage was achieved using standard coupling procedures (Löfås and Johnsson, 1990). Briefly, CM5 sensor chips were activated by injecting 35 μl of a 1:1 mixture of N-ethyl-N'-[dimethylamino]carbodiimide/N-hydroxysuccinimide at 5 $\mu\text{l}/\text{min}$. After diluting the proteins in 10 mM sodium acetate (pH 5.5), PKA (with HSA as a control) was coupled to the CM5 sensor chip by injecting a 50 μM solution of the protein selected with a flow rate of 5 $\mu\text{l}/\text{min}$ until 11,000 RU was reached.

Generation of Kinetic Binding Data

Kinetic studies with a range of analyte concentrations were determined at a flow rate of 10 $\mu\text{l}/\text{min}$ by allowing 300 s for association and 900 s for dissociation. Analytes were diluted in MilliQ water or running buffer (50 mM MOPS [pH 7.4], 50 mM KCl, and 10 mM MgCl_2). Kinetic data were analyzed with BIAevaluation 3.0 software. For each binding curve, the response obtained using the HSA cell as control was subtracted. Due to the small signals (up to 40 RU), the steady-state affinity model was used to determine the K_d of the different small molecular weight compounds. Goodness of fit (measured as χ^2) was less than 5 for binding of the low molecular weight compounds. All binding experiments were repeated two times, and biosensor chips coupled at different times yielded surfaces with identical binding affinities. The binding affinities of H-1152P, HA-1077, and Y-27632 to PKA were similar to the K_d values reported in different studies (Sasaki et al., 2002; Uehata et al., 1997) and citations therein, using enzymatic assays.

Data Collection and Structure Determination

Diffraction data were measured at 4°C in a sealed capillary on an image plate detector (Mar research) or Bruker X1000 area detector using a copper target Rigaku Rotaflex X-ray generator and graphite crystal K_α monochromator. In each case one crystal was sufficient to obtain a complete data set. The data were processed with the programs MOSFLM and SCALA or ASTRO and SAINT. All crystals have an orthorhombic symmetry ($P2_12_12_1$) with similar cell constants (Table 1). The structures were determined by molecular replacement using the CCP4 program package (www.ccp4.ac.uk/main/html). As a starting model we chose a PKA structure in a closed conformation (our unpublished data). Refmac 5.1.24 was used for refinement, while MOLOC was used (www.moloc.ch) for graphical evaluation and model building.

Surface Calculations

Buried surfaces were calculated with the program Insight II (Accelrys). The total surface of the isolated inhibitor and the accessible surface of the inhibitor in the complex were calculated. The difference is the buried surface.

Sequence Alignment and Homology Model Building

Sequences were aligned using the ClustalW server from <http://www.ebi.ac.uk/clustalw/>. The homology model was calculated by the SWISS-MODEL Protein Modelling Server (<http://www.expasy.ch/swissmod/SWISS-MODEL.html>).

Acknowledgments

We thank Norbert König for expert technical assistance and Wolf Lehmann for verifying enzyme purity by mass spectrometry.

Received: May 30, 2003

Revised: August 14, 2003

Accepted: August 14, 2003

Published: December 2, 2003

References

- Akamine, P., Madhusudan, Wu, J., Xuong, N.H., Eyck, L.F.T., and Taylor, S.S. (2003). Dynamic features of cAMP-dependent protein kinase revealed by apoenzyme crystal structure. *J. Mol. Biol.* 327, 159–171.
- Amano, M., Ito, M., Kimura, K., Fukata, Y., Chihara, K., Nakano, T., Matsuura, Y., and Kaibuchi, K. (1996). Phosphorylation and activa-

- tion of myosin by Rho-associated kinase (Rho-kinase). *J. Biol. Chem.* 271, 20246–20249.
- Amano, M., Fukata, Y., and Kaibuchi, K. (2000). Regulation and functions of Rho-associated kinase. *Exp. Cell Res.* 267, 44–51.
- Battistutta, R., Sarno, S., De Moliner, E., Papinutto, E., Zanotti, G., and Pinna, L.A. (2000). The replacement of ATP by the competitive inhibitor emodin induces conformational modifications in the catalytic site of protein kinase CK2. *J. Biol. Chem.* 275, 29618–29622.
- Bossemeyer, D., Engh, R.A., Kinzel, V., Ponstingl, H., and Huber, R. (1993). Phosphotransferase and substrate binding mechanism of the cAMP-dependent protein kinase catalytic subunit from porcine heart as deduced from the 2.0 Å structure of the complex with Mn²⁺ adenylyl imidodiphosphate and inhibitor peptide PKI(5–24). *EMBO J.* 12, 849–859.
- Davies, S.P., Reddy, H., Caivano, M., and Cohen, P. (2000). Specificity and mechanism of action of some commonly used protein kinase inhibitors. *Biochem. J.* 357, 95–105.
- Engh, R.A., and Bossemeyer, D. (2001). The protein kinase activity modulation sites: mechanisms for cellular regulation—targets for therapeutic intervention. *Adv. Enzyme Regul.* 47, 121–149.
- Engh, R.A., and Bossemeyer, D. (2002). Structural aspects of protein kinase control: role of conformational flexibility. *Pharmacol. Ther.* 93, 99–111.
- Engh, R.A., Girod, A., Kinzel, V., Huber, R., and Bossemeyer, D. (1996). Crystal structures of catalytic subunit of cAMP-dependent protein kinase in complex with isoquinolinesulfonyl protein kinase inhibitors H7, H8, and H89. Structural implications for selectivity. *J. Biol. Chem.* 271, 26157–26164.
- Fukata, Y., Amano, M., and Kaibuchi, K. (2001). Rho-Rho-kinase pathway in smooth muscle contraction and cytoskeletal reorganization of non-muscle cells. *Trends Pharmacol. Sci.* 22, 32–39.
- Gassel, M., Breitenlechner, C.B., Ruger, P., Jucknischke, U., Schneider, T., Huber, R., Bossemeyer, D., and Engh, R.A. (2003). Mutants of protein kinase A that mimic the ATP-binding site of protein kinase B (AKT). *J. Mol. Biol.* 329, 1021–1034.
- Gibbs, C.S., Knighton, D.R., Sowadski, J.M., Taylor, S.S., and Zoller, M.J. (1992). Systematic mutational analysis of cAMP-dependent protein kinase identifies unregulated catalytic subunits and defines regions important for the recognition of the regulatory subunit. *J. Biol. Chem.* 267, 4806–4814.
- Hidaka, H., Inagaki, M., Kawamoto, S., and Sasaki, Y. (1984). Isoquinolinesulfonamides, novel and potent inhibitors of cyclic nucleotide dependent protein kinase and protein kinase C. *Biochemistry* 23, 5036–5041.
- Ikenoya, M., Hidaka, H., Hosoya, T., Suzuki, M., Yamamoto, N., and Sasaki, Y. (2002). Inhibition of Rho-kinase-induced myristoylated alanine-rich C kinase substrate (MARCKS) phosphorylation in human neuronal cells by H-1152, a novel and specific Rho-kinase inhibitor. *J. Neurochem.* 87, 9–16.
- Ishizaki, T., Uehata, M., Tamechika, I., Keel, J., Nonomura, K., Maekawa, M., and Narumiya, S. (2000). Pharmacological properties of Y-27632, a specific inhibitor of Rho-associated kinases. *Mol. Pharmacol.* 57, 976–983.
- Itoh, K., Yoshioka, K., Akedo, H., Uehata, M., Ishizaki, T., and Narumiya, S. (1999). An essential part for Rho-associated kinase in the transcellular invasion of tumor cells. *Nat. Med.* 5, 221–225.
- Johnson, D.A., Akamine, P., Radzio-Andzelm, E., Madhusudan, and Taylor, S.S. (2001). Dynamics of cAMP-dependent protein kinase. *Chem. Reviews* 101, 2243–2270.
- Lófás, S., and Johnsson, B. (1990). A novel hydrogel matrix on gold surfaces in surface plasmon resonance sensors for fast and efficient covalent immobilization of ligands. *J. Chem. Soc. Chem. Commun.* 21, 1526–1528.
- Manning, G., Whyte, D.B., Martinez, R., Hunter, T., and Sudarsanam, S. (2002). The protein kinase complement of the human genome. *Science* 298, 1912–1934.
- Matsui, T., Amano, M., Yamamoto, T., Chihara, K., Nakafuku, M., Ito, M., Nakano, T., Okawa, K., Iwamatsu, A., and Kaibuchi, K. (1996). Rho-associated kinase, a novel serine threonine kinase, as a putative target for the small GTP binding protein Rho. *EMBO J.* 15, 2208–2216.
- Narayana, N., Diller, T.C., Koide, K., Bunnage, M.E., Nicolaou, K.C., Brunton, L.L., Xuong, N.H., Ten Eyck, L.F., and Taylor, S.S. (1999). Crystal structure of the potent natural product inhibitor balanol in complex with the catalytic subunit of cAMP-dependent protein kinase. *Biochemistry* 38, 2367–2376.
- Ono-Saito, N., Niki, I., and Hidaka, H. (1999). H-series protein kinase inhibitors and potential clinical applications. *Pharmacol. Ther.* 82, 123–131.
- Orellana, S.A., Amieux, P.S., Zhao, X., and McKnight, G.S. (1993). Mutations in the catalytic subunit of the cAMP-dependent protein kinase interfere with holoenzyme formation without disrupting inhibition by protein kinase inhibitor. *J. Biol. Chem.* 268, 6843–6846.
- Prade, L., Engh, R.A., Girod, A., Kinzel, V., Huber, R., and Bossemeyer, D. (1997). Staurosporine-induced conformational changes of cAMP-dependent protein kinase catalytic subunit explain inhibitory potential. *Structure* 5, 1627–1637.
- Sasaki, Y., Suzuki, M., and Hidaka, H. (2002). The novel and specific Rho-kinase inhibitor (S)-(+)-2-methyl-1-[(4-methyl-5-isoquinoline)sulfonyl]-homopiperazine as a probing molecule for Rho-kinase-involved pathway. *Pharmacol. Ther.* 93, 225–232.
- Shimokawa, H., Iinuma, H., Kishida, H., Nakashima, M., and Kato, K. (2001). Antianginal effect of fasudil, a Rho-kinase inhibitor, in patients with stable effort angina: a multicenter study. *Circulation* 104, 2843.
- Sinnett-Smith, J., Lunn, J.A., Leopoldt, D., and Rozengurt, E. (2001). Y-27632, an inhibitor of Rho-associated kinases, prevents tyrosine phosphorylation of focal adhesion kinase and paxillin induced by bombesin: dissociation from tyrosine phosphorylation of p130(CAS). *Exp. Cell Res.* 266, 292–302.
- Tanaka, H., Ohshima, N., Takagi, M., Komeima, K., and Hidaka, H. (1998). Novel vascular relaxant, Hmn-1152: its molecular mechanism of action. *Naunyn-Schmied. Arch. Pharmacol.* 358, P3740.
- Trauger, J.W., Lin, F.F., Turner, M.S., Stephens, J., and LoGrasso, P.V. (2002). Kinetic mechanism for human Rho-Kinase II (ROCK-II). *Biochemistry* 41, 8948–8953.
- Uehata, M., Ishizaki, T., Satoh, H., Ono, T., Kawahara, T., Morishita, T., Tamakawa, H., Yamagami, K., Inui, J., Maekawa, M., and Narumiya, S. (1997). Calcium sensitization of smooth muscle mediated by a Rho-associated protein kinase in hypertension. *Nature* 389, 990–994.
- Yang, J., Cron, P., Good, V.M., Thompson, V., Hemmings, B.A., and Barford, D. (2002). Crystal structure of an activated Akt/protein kinase B ternary complex with GSK3-peptide and AMP-PNP. *Nat. Struct. Biol.* 9, 940–944.

Accession Numbers

Atomic coordinates have been deposited in the Protein Data Bank with accession numbers 1Q8T, 1Q8U, and 1Q8W.

REVIEWS

GLIVEC (STI571, IMATINIB), A RATIONALLY DEVELOPED, TARGETED ANTICANCER DRUG

Renaud Capdeville, Elisabeth Buchdunger, Juerg Zimmermann and Alex Matter

In the early 1980s, it became apparent that the work of pioneers such as Robert Weinberg, Mariano Barbacid and many others in identifying cancer-causing genes in humans was opening the door to a new era in anticancer research. Motivated by this, and by dissatisfaction with the limited efficacy and tolerability of available anticancer modalities, a drug discovery programme was initiated with the aim of rationally developing targeted anticancer therapies. Here, we describe how this programme led to the discovery and continuing development of Glivec (Gleevec in the United States), the first selective tyrosine-kinase inhibitor to be approved for the treatment of a cancer.

LEUKAEMIA

Leukaemia is an uncontrolled proliferation of one type of white blood cell (leukocyte).

Until the early 1980s, drug discovery programmes for cancer were focused almost exclusively on DNA synthesis and cell division, and resulted in agents such as antimetabolites, alkylating agents and microtubule destabilizers. These drugs showed efficacy, but at the price of high toxicity due to lack of selectivity. Also, resistance was frequently observed after initial stabilization or regression of the disease. The discovery of cancer-causing genes, later called oncogenes, represented a radical departure — all of a sudden, genes were identified that were uniquely associated with cancerous cells. The molecular epidemiology of these genes was established over many years of studying clinical tumour samples, but as described below, it was clear at the outset that chronic myelogenous LEUKAEMIA (CML) — a haematological stem-cell disorder that is characterized by excessive proliferation of cells of the myeloid lineage — represented a particularly interesting case.

Target selection: BCR-ABL

CML is characterized by a reciprocal translocation between chromosomes 9 and 22 (REF. 1). The shortened version of chromosome 22, which is known as the Philadelphia chromosome, was discovered by Nowell and Hungerford², and provided the first evidence of a specific genetic change associated with human cancer.

The molecular consequence of this inter-chromosomal exchange is the creation of the *BCR-ABL* gene, which encodes a protein with elevated tyrosine-kinase activity. The demonstration that *Bcr-Abl* as the sole oncogenic event could induce leukaemias in mice^{3–5} has established *BCR-ABL* as the molecular pathogenic event in CML. As the tyrosine-kinase activity of *BCR-ABL* is crucial for its transforming activity⁶, the enzymatic activity of this deregulated gene could plausibly be defined as an attractive drug target for addressing *BCR-ABL*-positive leukaemias.

For the first time, a drug target was identified that clearly differed in its activity between normal and leukaemic cells. It was conceivable that this enzyme could be approached with classical tools of pharmacology, as its activity — the transfer of phosphate from ATP to tyrosine residues of protein substrates — could clearly be described and measured in biochemical as well as cellular assays. Furthermore, cell lines that were derived from human leukaemic cells with the same chromosomal abnormality were available. Such cell lines were instrumental for *in vitro* and animal studies, which laid the groundwork for the clinical trials. So, the essential tools were assembled to go forward with the aim of identifying potent and selective inhibitors of the *ABL* tyrosine kinase.

Novartis Oncology, Novartis
Pharma AG, S-27 2.033,
CH-4002 Basel,
Switzerland.
Correspondence to R.C.
e-mail: renaud.capdeville@
pharma.novartis.com
doi:10.1038/nrd839

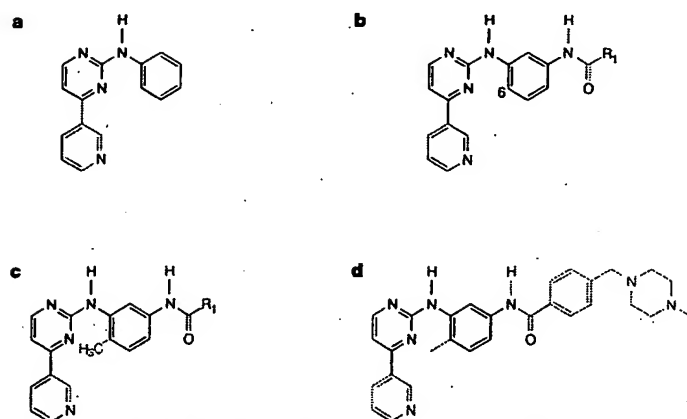


Figure 1 | Summary of the chemical optimization. The core structure of the lead compound, a phenylamino derivative, is indicated in black. **a** | The addition of a 3'-pyridyl group (blue) at the 3'-position of the pyrimidine enhanced the cellular activity. **b** | An amide group (red) attached to the phenyl ring provided activity against tyrosine kinases. **c** | A 'flag methyl' (purple) attached to the diaminophenyl ring abolished the undesirable protein-kinase-C inhibitory activity. **d** | The final attachment of an *N*-methyl piperazine moiety (green) markedly increased the solubility and oral bioavailability.

Medicinal chemistry

The starting point for every medicinal-chemistry project is a lead compound with a given pharmacological activity. However, the biological activity of a molecule must be complemented by other properties that make the molecule a good drug — it is estimated that a large proportion of molecules fails in late stages of drug development due to drug–drug interactions or poor ADME (absorption, distribution, metabolism and excretion) features. Not detecting these liabilities early in the drug discovery process can be extremely costly and time consuming. On the basis of physical and calculated properties for known drugs, criteria for 'drug-likeness' have been established⁷.

In the case of Glivec, a lead compound was identified in a screen for inhibitors of protein kinase C (PKC). This compound — a phenylaminopyrimidine derivative — had promising 'lead-like' properties⁸ and a high potential for diversity, allowing simple chemistry to be applied to produce compounds with more potent activity or selectivity. Strong PKC inhibition in cells was obtained with derivatives bearing a 3'-pyridyl group at the 3'-position of the pyrimidine (FIG. 1a). During the optimization of this structural class, it was observed that the presence of an amide group on the phenyl ring provided inhibitory activity against tyrosine kinases, such as the BCR–ABL kinase (FIG. 1b). At this point, a key observation from analysis of structure–activity relationships was that a substitution at position 6 of the diaminophenyl ring abolished PKC inhibitory activity completely. Indeed, although the introduction of a simple 'flag-methyl' led to loss of activity against PKC, the activity against protein tyrosine kinases was retained or even enhanced (FIG. 1c). However, the first series of selective inhibitors that was prepared originally showed poor oral bioavailability

and low solubility in water. The attachment of a highly polar side chain (an *N*-methylpiperazine) was found to improve markedly both solubility and oral bioavailability. To avoid the mutagenic potential of aniline moieties, a spacer was introduced between the phenyl ring and the nitrogen atom. The best compound from this series was a methylpiperazine derivative that was originally named ST1571 (imatinib, now known as Glivec or Gleevec), which was selected as the most promising candidate for clinical development^{9,10} (FIG. 1d).

Docking studies¹¹ and X-ray crystallography¹² showed that binding of Glivec occurs at the ATP-binding site. Analysis of the crystal structure¹² showed that Glivec inhibits the ABL kinase by binding with high specificity to an inactive form of the kinase. The need for the kinase to adopt this unusual conformation, which favours binding, might contribute to the high selectivity of the compound. Unexpectedly, these analyses indicated that the *N*-methylpiperazine group (added to increase drug solubility) also interacted strongly with ABL by means of hydrogen bonds to the backbone carbonyl group of isoleucine (Ile)360 and histidine (His)361.

In an *in vitro* screen against a panel of protein kinases, the compound was found to inhibit the autophosphorylation of essentially three kinases: BCR–ABL, c-KIT and the platelet-derived growth factor (PDGF) receptor (TABLE 1). More recently, activity against ARG kinase has also been reported¹³.

Pharmacological profile

In collaboration with Brian Druker, the selective inhibitory activity of Glivec was shown at the cellular level on the constitutively active p210^{BCR–ABL} tyrosine kinase¹⁴. Subsequently, a similar inhibitory activity was also shown on other ABL fusion proteins, such as p185^{BCR–ABL} (REFS 15,16) and TEL (ETV6)–ABL¹⁵. The inhibition of autophosphorylation of BCR–ABL was closely related to the antiproliferative activity of Glivec. Incubation with submicromolar concentrations of Glivec selectively induced APOPTOSIS in BCR–ABL-positive cell lines, and induced cell killing in primary leukaemia cells from patients with Philadelphia-chromosome-positive (Ph⁺) CML and acute lymphoblastic leukaemia^{14,16–20}.

In *in vivo* experiments, once daily intraperitoneal treatment with 2.5–50 mg kg^{−1} of Glivec, started one week after injecting BCR–ABL-transformed 32D cells into SYNGENEIC mice, caused dose-dependent inhibition of tumour growth¹⁴. In nude mice implanted with KU812 cells, oral treatment with 160 mg kg^{−1} daily in three divided doses for 11 consecutive days was associated with continuous blockage of p210^{BCR–ABL} tyrosine phosphorylation, and resulted in tumour-free survival of the animals²⁰. The antitumour effect of Glivec was specific for BCR–ABL-expressing cells, as no growth inhibition occurred in mice that were given injections of U937, a BCR–ABL-negative myeloid cell line. Recently, Glivec was shown to be orally active in a mouse model of CML, based on retroviral p210^{BCR–ABL}

APOPTOSIS
Programmed cell death.

SYNGENEIC MODEL
An animal model in which the injected tumour cells are derived from the same animal species as the host animal.

transduction of transplanted bone marrow. Survival of animals was significantly prolonged, together with a marked improvement in peripheral-white-blood-cell counts and splenomegaly²¹.

Table 1 | Cellular profile of Glivec

Assay	IC ₅₀ (μM)
Inhibition of autophosphorylation	
v-ABL	0.1–0.3
p210 ^{BCR-ABL}	0.25
p185 ^{BCR-ABL}	0.25
TEL-ABL	0.35
TEL-ARG	0.5
PDGF receptor	0.1
TEL-PDGF receptor	0.15
c-KIT	0.1
FLT3	> 10
c-FMS and v-fms	> 10
EGF receptor	> 100
c-ERBB2	> 100
Insulin receptor	> 100
IGF-1 receptor	> 100
v-SRC	> 10
JAK2	> 100
Inhibition of MAPK activation	
PDGF dependent	0.1–1
SCF dependent	0.1–1
Inhibition of AKT activation	
SCF dependent	0.1–1
Inhibition of IP release	
PDGF induced	0.25
Inhibition of c-FOS mRNA expression	
PDGF induced	0.3–1
EGF, FGF or PMA induced	> 100
Antiproliferative activity*	
32D, MO-7e, BaF3 cells	> 10
BCR-ABL-transfected 32D, MO-7e, BaF3 cells	< 1
BCR-ABL-positive human leukaemia lines [†]	0.1–1
BaF3 TEL-ARG	0.5
BALB/c 3T3 v-SIS (PDGF autocrine)	0.3
BaF3 TEL-PDGF receptor	< 1
U-87 human glioma [‡]	~1.5
U-343 human glioma [‡]	~1.5
MO-7e, SCF stimulated	~0.1
H526 human SCLC, SCF stimulated [§]	0.8
Human GIST882 line [¶]	< 1
Human mast-cell leukaemia line HMC-1 [¶]	0.01–0.1

Glivec concentrations that cause 50% inhibition (IC₅₀) are given^{13–20,47,48,53,54,61,63,66}. EGF, epidermal growth factor; FGF, fibroblast growth factor; FLT3, fms-related tyrosine kinase 3; IGF-1, insulin-like growth factor-1; IP, inositol phosphate; MAPK, mitogen-activated protein kinase; PDGF, platelet-derived growth factor; PMA, phorbol 12-myristate 13-acetate; SCF, stem-cell factor; SCLC, small-cell lung cancer. *Antiproliferative experiments were carried out in 10% fetal calf serum, except for those that were carried out in 5% human-platelet poor plasma or under [§]serum-free conditions. [†]K562, KU812, MC-3, MBA-1, KBM-5, Z-33, Z-119, Z-181. [‡]Expresses the activating KIT mutation K642E (lysine 642 to glutamic acid). [¶]Expresses the activating KIT mutation V560G (valine 560 to glycine).

Fundamental phenotypic features in BCR-ABL-positive cells involve resistance to apoptosis, enhanced proliferation and altered adhesion properties. The impact of Glivec on some known downstream signalling molecules of BCR-ABL has been examined. A link between constitutive activation of STAT5 (signal transducer and activator of transcription 5) and enhanced viability of BCR-ABL-transformed cells has been shown^{22,23}. Glivec had a profound inhibitory effect on STAT5 activation *in vitro* and *in vivo*^{21–23}. Furthermore, inhibition of the BCR-ABL kinase activity by Glivec in BCR-ABL-expressing cell lines and fresh leukaemic cells from CML patients induced apoptosis by suppressing the capacity of STAT5 to activate the expression of the anti-apoptotic protein BCL-X_L²³. The adaptor molecule CRKL is a prominent target of BCR-ABL, and its tyrosine phosphorylation has been a useful marker of BCR-ABL kinase activity²⁴. As expected, a decrease in tyrosine phosphorylation of CRKL has been observed in Glivec-treated cell lines, and has also served as an indicator of BCR-ABL kinase activity in patients (see below).

There is increasing evidence that cell-cycle regulation is disturbed in BCR-ABL-positive cells; however, the underlying molecular mechanisms are poorly understood. Recently, BCR-ABL has been shown to promote cell-cycle progression and activate cyclin-dependent kinases by interfering with the regulation of the cell-cycle inhibitory protein p27 (REF. 25). Glivec prevented downregulation of p27 levels in BCR-ABL-expressing cells^{25,26}.

The effects of Glivec on cytoskeletal changes and adhesion have been investigated using BCR-ABL-transfected fibroblasts²⁷. Glivec was shown to restore normal architecture and to increase adhesion in this model of BCR-ABL expression.

Clinical development in CML

Because of the three known targets of Glivec, many potential cancers can be speculated to be good candidates for clinical testing of this new drug. However, in most cancers, tumorigenesis is complex and involves the disruption of multiple genes and signalling pathways. By contrast, CML can be considered as one of the few examples of a malignancy in which a single signalling-pathway defect is thought to cause the disease. In addition, in contrast to most of the solid tumours, for which the measurement of tumour response is complex, pharmacodynamic response in CML can be measured easily using blood leukocyte count as the end point. For these reasons, CML was selected as the first indication for Phase I clinical testing.

Clinically, CML is a chronic disease that evolves through three successive stages, from the chronic phase to the end stage of blast crisis that resembles acute leukaemia (FIG. 2). Overall, the median survival time of patients with newly diagnosed CML is approximately 5–6 years with an interferon-based treatment regimen. The first trial with Glivec was a Phase I study in patients with chronic-phase, and subsequently also with blast-phase, CML. In this trial, patients were treated with doses

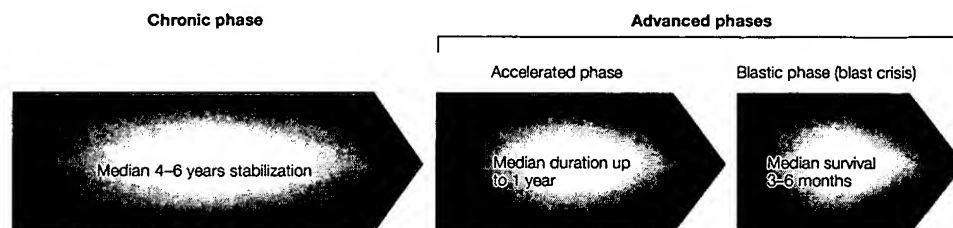


Figure 2 | Clinical course of chronic myelogenous leukaemia.

ranging from 25 to 1,000 mg per day, and no maximal tolerated dose was identified, despite a trend for a higher frequency of GRADE III–IV ADVERSE EVENTS at doses of 750 mg or higher. On the other hand, a clear dose–response relationship with respect to efficacy was described in patients with chronic-phase CML. At doses of 300 mg or higher, 98% of the patients achieved a complete haematological response, and trough serum levels were above the concentrations required for *in vitro* activity^{28,29}. Subsequently, a mathematical modelling of the relationship between dose and response, as measured by leukocyte counts after four weeks of therapy, confirmed that doses of 400 mg and higher were optimal in inducing a haematological response³⁰ (FIG. 3). In addition, effective inhibition of the BCR–ABL kinase was documented in patient samples by inhibition of the phosphorylation status of the downstream target CRKL²⁷. From this study, doses ranging from 400 mg (for chronic-phase patients) to 600 mg (for advanced-phase CML) were recommended for subsequent studies.

Subsequently, three large multinational studies have been carried out in 532 patients with late chronic-phase CML in whom previous interferon therapy had failed³¹, in 235 patients with accelerated-phase CML³², and in 260 patients with myeloid blast crisis³³. Treatment was given at a dose of 400 mg in the chronic-phase trial and 600 mg in the two other studies. The results of these three studies indicated that the rate of both haematological and cytogenetic response increased as the treatment was started earlier in the course of the disease (FIG. 4). Importantly, the achievement of a haematological and/or cytogenetic response was associated with improved survival and progression-free survival^{31–33}. In the chronic-phase study, in which patients started treatment within a median of 32 months after their initial diagnosis, the estimated probability of being free of progression at 18 months was 89.2%³¹. The most frequently reported adverse events were mild nausea, vomiting, oedema and muscle cramps. However, rare but serious adverse events, such as liver

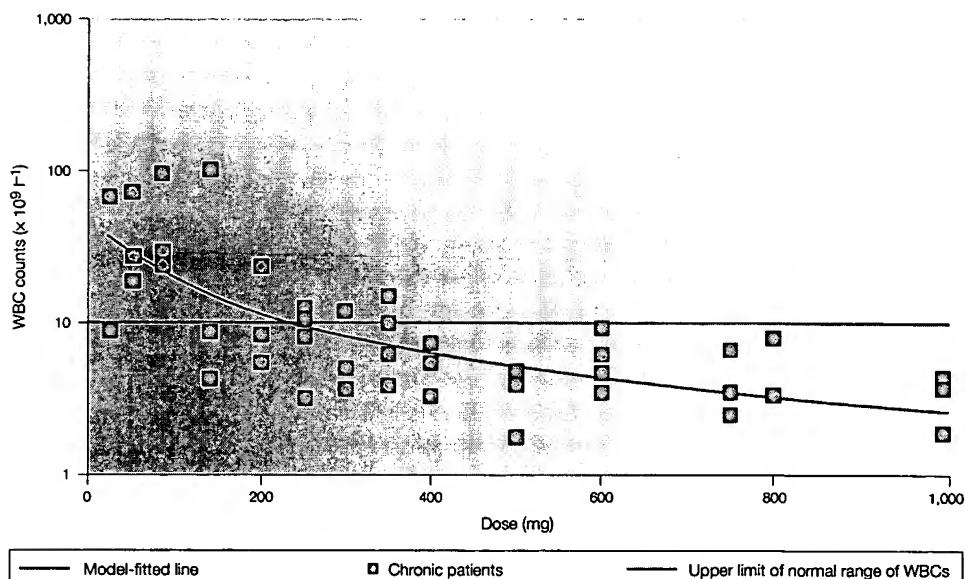


Figure 3 | **Dose–response relationship of Gleevec in CML (Phase I study).** Using the leukocyte (white blood cell; WBC) count after 28 days of treatment as a pharmacodynamic marker, the relationship between dose and response was modelled using an E_{max} model, which makes the assumption that once the maximal effect is achieved (E_{max}), increasing the dose further does not translate into additional benefit. The data indicate that at doses of 400 mg per day or higher, all the patients are predicted to achieve a reduction of their leukocyte counts within normal range below $10 \times 10^9 \text{ l}^{-1}$. Adapted with permission from REF. 30 © (2001) American Society of Clinical Oncology. CML, chronic myelogenous leukaemia.

GRADE III–IV ADVERSE EVENTS
For each adverse event that is associated with a specific treatment, grades are assigned and defined using a scale from 0 to V. Grade III, severe and undesirable adverse event; grade IV, life-threatening or disabling adverse event.

toxicity or fluid-retention syndromes, were also reported. Neuropaenias and thrombopaenias were more common in patients with advanced disease, which indicates that haematological toxicity might be related more to an underlying compromised bone-marrow reserve than to toxicity of the drug itself through inhibition of c-KIT-driven haematopoiesis. Taken together, these findings have established Glivec as a safe and effective therapy in all stages of CML, and were the basis for marketing approval by the FDA on 10 May 2001 — less than three years after the start of the first Phase I study (FIG. 5).

Resistance. In CML blast crisis, even though the rate of haematological responses with Glivec is high, these responses are usually short lived, and most patients will ultimately develop resistance and undergo disease progression. A prerequisite to optimally develop strategies to prevent or overcome this resistance is to get a good understanding of the potential mechanisms of resistance in these patients.

On the basis of preclinical and clinical data that are available at present, several potential mechanisms of resistance have been described, which are summarized in BOX 1. They can be categorized into two main groups: mechanisms whereby BCR-ABL is reactivated and cell proliferation remains dependent on BCR-ABL signalling, and mechanisms whereby the BCR-ABL protein remains inhibited by Glivec, but alternative signalling pathways become activated.

BCR-ABL overexpression and BCR-ABL gene amplification has been shown in p210^{BCR-ABL}-transformed mouse haematopoietic Ba/F3 cells that are resistant to Glivec^{34,35}, as well as in human BCR-ABL-positive leukaemia lines LAMA84 and AR230 (REFS 35,36).

In treated patients, there is now increasing evidence that amplification of the BCR-ABL gene and mutations in the BCR-ABL kinase domain are two common mechanisms of resistance to Glivec. The occurrence of these mechanisms was first reported by Sawyers' group³⁷. In a study of 11 patients with blast crisis and overt clinical resistance when treated with Glivec, 3 had amplification of the BCR-ABL gene and 6 had a point mutation in the ABL kinase domain, which resulted in a T315I (threonine 315 to isoleucine) amino-acid substitution. Following this initial report, the T315I mutation as well as further mutations in the ABL kinase domain have been reported by various investigators³⁸⁻⁴¹. Even though these mutations vary in their type and frequency, it is speculated that they might all lead to a reactivation of BCR-ABL-driven signal transduction. To understand the molecular mechanism by which such mutations might cause resistance to Glivec, current studies are using X-ray crystallography to analyse the three-dimensional structure of a complex between the drug and the human c-ABL kinase domain. Glivec binds to an unusual, inactive conformation of ABL with the amino terminus of the activation loop, which contains the highly conserved DFG (asparagine-phenylalanine-glycine) motif, folded into the ATP-binding site⁴². This conformation has been

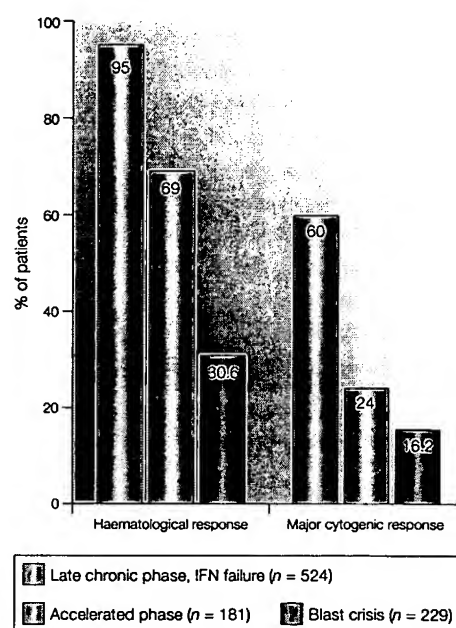
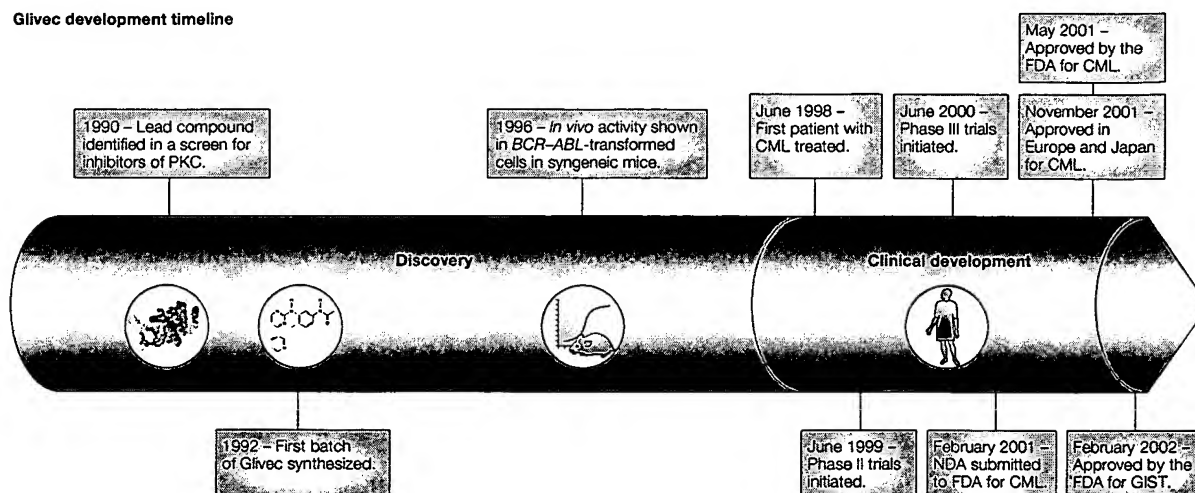


Figure 4 | Haematological and cytogenetic response in CML: Phase II data. In all studies, results are expressed as the percentage of responding patients among the patients for whom the diagnosis of the correct phase of chronic myelogenous leukaemia (CML) was confirmed after a central review of the data. A major cytogenetic response combines both complete (0% Ph⁺ metaphases) and partial (1–35% Ph⁺) responses. Haematological response was defined as complete haematological response (CHR) in the chronic-phase study, and as either a CHR, a marrow response or a return to chronic phase (RTC) in the advanced-phase studies, all to be confirmed after at least four weeks. In the chronic-phase study, CHR was defined as white blood cells $<10 \times 10^9 \text{ l}^{-1}$, platelets $<450 \times 10^9 \text{ l}^{-1}$, myelocytes and metamyelocytes $<5\%$ in blood, no blasts and promyelocytes in blood, basophils $<20\%$ and no extramedullary involvement. In advanced-phase studies, CHR was defined as neutrophils $= 1.5 \times 10^9 \text{ l}^{-1}$, platelets $= 100 \times 10^9 \text{ l}^{-1}$, no blood blasts, marrow blasts $<5\%$ and no extramedullary disease. A marrow response was defined by the same criteria as for CHR, but with neutrophils $= 1 \times 10^9 \text{ l}^{-1}$ and platelets $= 20 \times 10^9 \text{ l}^{-1}$. An RTC was defined as $<15\%$ blasts in marrow and blood, $<30\%$ blasts and promyelocytes in marrow and blood, $<20\%$ basophils in blood and no extramedullary disease. IFN, interferon; Ph⁺, Philadelphia chromosome positive.

observed by Kuriyan and co-workers¹² in a complex between mouse c-Abl and a Glivec analogue, and cannot bind ATP. The knowledge of the crystal structure allows a better understanding of the decreased sensitivity of mutated BCR-ABL to Glivec, and can be a powerful tool in the design of new BCR-ABL inhibitors that maintain inhibitory activity against these mutated kinases.

Resistance to Glivec might also be related to pharmacokinetic factors. Glivec is a substrate of the multi-drug-resistance-associated P-glycoprotein (PgP).

Glivec development timeline



Typical development timeline

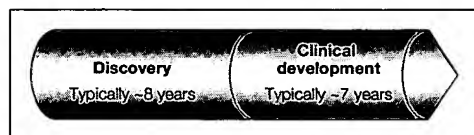


Figure 5 | Key points in the discovery and development of Glivec. The clinical development was particularly rapid, as can be seen by comparison with the typical drug discovery and development times shown in the inset. An NDA for Glivec was submitted just two years and nine months after treatment of the first patient with CML, and FDA approval was given less than three months after application. CML, chronic myelogenous leukaemia; GIST, gastrointestinal stromal tumour; NDA, new drug application; PKC, protein kinase C.

Accordingly, the uptake of Glivec was reduced in Glivec-resistant LAMA84 cells in association with an overexpression of the PgP protein. Sensitivity to Glivec was recovered when cells were treated with the PgP inhibitor verapamil³⁵. At clinically relevant concentrations of Glivec, binding to plasma proteins is approximately 95%, mostly to albumin and α 1-acid glycoprotein (AGP). It has been suggested that a potential mechanism of resistance might relate to this high binding to increased levels of AGP, which would lead to insufficient availability of free drug for antileukaemic activity⁴³. However, the clinical significance of this hypothesis is uncertain, in particular in view of the finding that AGP purified from CML patients failed to block the effect of Glivec on the proliferation of leukaemic cells⁴⁴.

Recently, Hofmann *et al.*⁴⁵ studied a small group of patients with Ph⁺ acute lymphoblastic leukaemia who were resistant to Glivec by using DNA-microarray expression profiling. They described an association between the occurrence of resistance to Glivec and upregulation of genes encoding proteins such as Bruton tyrosine kinase and two ATP synthetases (ATP5A1 and ATP5C1), and downregulation of other genes, such as the pro-apoptotic gene *BAK1* and the cell-cycle-control gene *INK4B*⁴⁶ (also known as *p15*). This is the first report to identify dysregulation of genes

that are unrelated to BCR-ABL signalling, and further studies will be necessary to fully assess the significance of these findings and their relevance to CML patients.

Current and future development in CML

The activity of Glivec in patients with newly diagnosed CML is being further investigated by a large randomized Phase III study to compare first-line therapy with Glivec against standard interferon in combination with low-dose cytarabine. This study, known as the 'IRIS' study (International Randomized study of Interferon versus ST1571), has enrolled 1,106 patients. The results of an interim analysis with a median follow-up of 14 months indicate a better tolerability and a superior efficacy of first-line Glivec compared with interferon and low-dose cytarabine in terms of cytogenetic response, haematological response and, more importantly, time to progression to accelerated phase or blast crisis⁴⁶.

Preclinical studies have shown that the combination of Glivec with various anticancer agents might have synergistic effects. Consequently, several Phase I/II studies are evaluating the feasibility of combining Glivec with interferon, polyethylene glycol (PEG)ylated interferon, cytarabine and other single-agent or combination chemotherapy regimens, in patients with either chronic-phase or advanced CML.

Box 1 | Mechanisms of resistance to Glivec in CML**BCR-ABL-dependent mechanisms (cells remain dependent on BCR-ABL signalling)**

- Amplification of *BCR-ABL* gene
- Mutations in BCR-ABL kinase domain prevent correct binding of Glivec
- Efflux of Glivec (for example, by Pgp-associated MDR protein)
- Protein binding of Glivec (for example, to circulating AGP)

BCR-ABL-independent mechanisms (BCR-ABL is inactivated)

- Activation of signalling pathways downstream of BCR-ABL
- Activation of leukaemogenic pathways unrelated to BCR-ABL

AGP, α 1-acid glycoprotein; CML, chronic myelogenous leukaemia; MDR, multidrug resistant; Pgp, P-glycoprotein.

c-KIT is another target

In addition to various oncogenic forms of the BCR-ABL tyrosine kinase, Glivec also inhibits the receptor for stem-cell factor (SCF) — c-KIT, a member of the type III group of receptor kinases. Preclinical studies have established that the drug blocks c-KIT autophosphorylation, as well as SCF-stimulated downstream signalling events, such as activation of the mitogen-activated protein kinases (MAPKs) ERK1 and ERK2, and AKT (also known as protein kinase B)^{47,48}.

Development in c-KIT-positive GISTs. Gastrointestinal stromal tumours (GISTs) represent a rare subset of soft-tissue sarcomas that involve the gastrointestinal tract and are thought to be derived from the interstitial cells of Cajal. Scientific rationale for the use of Glivec in the treatment of these tumours comes from the landmark work of Hirota *et al.*⁴⁹, who first identified somatic gain-of-function mutations in the *c-KIT* gene in patients with GIST. Oncogenic *c-KIT* mutations in GISTs have been localized to the extracellular domain, kinase domains 1 and 2 and predominantly in the juxtamembrane domain of the c-KIT protein^{50–52}. As c-KIT serves as a phenotypic marker of GISTs and has a key role in their pathogenesis, it provides an ideal target for molecular-based therapy. The first evidence that Glivec might inhibit GIST cells that express mutated *c-KIT* was obtained from studies in a mast-cell leukaemia line expressing a mutated *c-KIT* similar to that found in GISTs^{48,53}. Furthermore, Glivec rapidly and completely abolished constitutive phosphorylation of c-KIT in the human cell line GIST882, which expresses an activating *c-KIT* mutation in the first part of the cytoplasmic split-tyrosine-kinase domain, and inhibited proliferation in this GIST line⁵⁴. Similarly, a primary GIST cell culture that expressed a *c-KIT* exon 11 juxtamembrane mutation was also inhibited by Glivec⁵⁴.

As reported recently, a pronounced tumour response was first observed in a single patient with progressing GIST⁵⁵. Following this case report, the high level of efficacy of Glivec in GIST has been shown in two subsequent Phase I (REF. 56) and Phase II studies (REF. 57). Two large Phase III studies are being carried out at present to compare the effectiveness of two doses of Glivec (400 mg or 800 mg daily). On the basis of the Phase II data, the FDA approved the use of Glivec for GISTs on 1 February 2002.

AUTOCRINE
Describes an agent secreted from a cell that acts on the cell in which it is produced.

PARACRINE
Describes an agent secreted from a cell that acts on other cells in the local environment.

Other c-KIT-expressing tumours. In human systemic mastocytosis, most cases show a point mutation in codon 17 of *c-KIT*, which results in a D816V (aspartic acid 816 to valine) amino-acid substitution in the kinase-2 domain of c-KIT. Interestingly, this mutated c-KIT is resistant to inhibition by Glivec^{53,58}.

Expression of c-KIT and SCF has been reported in a retrospective small-cell lung cancer (SCLC) series, indicating that SCLC growth might involve an AUTOCRINE loop. Inhibition of c-KIT activation by transfection of a dominant-negative *c-KIT* gene results in loss of growth-factor independence^{59,60}. Furthermore, the c-KIT/PDGF-receptor inhibitor AG1296 inhibits growth of SCLC cells in serum-containing medium⁶⁰. In H526 SCLC cells, pretreatment with Glivec inhibited SCF-mediated c-KIT activation with an IC₅₀ (half-maximal inhibitory concentration) of 0.1 μ M (REF. 61). The compound also blocked downstream signal transduction, as evidenced by inhibition of SCF-mediated activation of MAPK and AKT, and potently inhibited SCF-mediated growth in serum-free medium, with a marked increase in apoptosis. Glivec also inhibited the growth of SCLC cell lines in a dose-dependent fashion when grown in serum-containing medium; however, the average IC₅₀ was in the range of 5 μ M (REFS 61,62).

Although *c-KIT* expression has been documented in various other human tumours, including acute myelogenous leukaemia, ovarian and testicular cancer, it will be important to determine the activation status of the receptor and its importance in the pathogenesis (for a review, see REF. 58). Furthermore, it needs to be explored whether pharmacological inhibition of PARACRINE or autocrine activation of this kinase will be successful therapeutically. Exploratory clinical studies are continuing at present in patients with *c-KIT*-expressing SCLC and acute myelogenous leukaemia.

PDGF receptor as a target

The third target of Glivec is the PDGF-receptor tyrosine kinase. Cellular studies have shown potent inhibition of the two structurally similar PDGF- α and PDGF- β receptors (PDGFR- α and PDGFR- β), as well as blockade of PDGF-mediated cellular events^{47,63}. PDGF is a connective-tissue-cell mitogen with *in vivo* functions that include embryonal development, wound healing and control of interstitial-fluid pressure in soft connective tissue. There is increasing evidence that the PDGF ligand-receptor system also has an important role in tumorigenesis⁶⁴. Paracrine and/or autocrine activation of the PDGFR kinase has been postulated in numerous malignancies, and the presence of PDGF autocrine loops is most well documented in gliomas⁶⁵. Glivec inhibited the *in vitro* and *in vivo* growth of cells with autocrine PDGF signalling, including the formation of tumours by the human glioblastoma lines U343 and U87, which had been injected into the brains of nude mice⁶⁶. The inhibitory effects were mediated predominantly through promotion of growth arrest rather than apoptosis.

Autocrine PDGFR activation is also well documented in tumour cells of dermatofibrosarcoma protuberans (DFSP), a highly recurrent, infiltrative skin tumour that is characterized by a chromosomal rearrangement involving chromosomes 17 and 22. The resulting fusion-gene product collagen I, $\alpha 1$ polypeptide (COL1A1)-PDGF- β triggers the autocrine stimulation of the PDGFR⁶⁷. COL1A1-PDGF β -transformed fibroblasts, as well as primary DFSP and giant-cell fibrosarcoma cell cultures, were inhibited by Glivec *in vitro* and *in vivo*⁶⁷⁻⁶⁹. The main mechanism by which Glivec affected DFSP tumour growth was through induction of apoptosis⁶⁹. Preliminary data indicate that Glivec might also be active in patients with DFSP⁷⁰.

Relatively little is known about the ligand-independent activation of PDGFR. However, rearrangement of PDGFR β has been described in chronic myeloproliferative diseases. The best known of these is the t(5;12) chromosomal translocation in chronic myelomonocytic leukaemia (CMML), in which PDGFR β , which is located on chromosome 5, is fused to the TEL gene on chromosome 12. Transformation of haematopoietic cells occurs through oligomerization of the TEL-PDGFR- β fusion protein, which causes ligand-independent constitutive activation of the PDGFR kinase⁷¹. Glivec inhibited the growth of cells expressing TEL-PDGFR β ⁷⁵, and in transgenic mice that expressed the TEL-PDGFR β , treatment with Glivec inhibited tumour formation and prolonged survival of the animals⁷². A remarkable haematological and complete cytogenetic response has been observed in two patients with chronic myeloproliferative disorders associated with a t(5;12) translocation — one of them with a well-characterized TEL-PDGFR fusion gene and the second with a rearranged PDGFR gene with an as yet unidentified partner gene⁷³. Other exploratory clinical trials are being carried out in gliomas and in prostate cancer.

Targeting the tumour microenvironment

An alternative strategy to influence tumour growth is to interfere with the tumour stroma and microvasculature. Paracrine PDGF signalling in the connective-tissue tumour stroma has been described in various types of solid tumour⁶⁴. Several lines of evidence indicate a role for PDGF in the regulation of interstitial fluid pressure (IFP)⁷⁴⁻⁷⁶. As most solid tumours have an increased IFP, pharmacological reduction might be a way to increase the uptake of anticancer drugs into tumours⁷⁷. Recent experiments have shown that Glivec significantly reduced tumour IFP in subcutaneously growing PRO rat-colon carcinomas, and a concomitant increase in *trans*-capillary transport of a radiolabelled tracer compound into the tumour interstitium was observed⁷⁸. These effects were mediated by inhibition of the expression of PDGFR on blood vessels and stromal cells, as tumour epithelial cells in this tumour model do not express PDGFRs.

The angiogenic activity that has been described for PDGF might not only be explained by its direct effects on capillary endothelial cells, pericytes and smooth-muscle

cells⁷⁹, but might also be influenced indirectly through paracrine action on PDGF-responsive stromal and perivascular cells, which are a principal source of vascular endothelial growth factor (VEGF)⁸⁰. PDGF has also been shown to induce the expression of VEGF in endothelial cells, which in turn causes an autocrine VEGF loop⁸¹. Anti-angiogenic activity of Glivec has been shown *in vitro* through inhibition of serum-stimulated capillary sprouting from rat aorta, and *in vivo* in a subcutaneous implant model in which the drug inhibited PDGF- and also VEGF- and basic fibroblast growth factor (bFGF)-stimulated vascularization⁸². Blockade of PDGFR signalling by Glivec has also been shown to inhibit angiogenesis and tumour growth in an experimental model of bone metastasis⁸³. Glivec treatment of nude mice injected with PC-3MM human prostate-cancer cells into the tibia inhibited tumour-cell growth and induced apoptosis, both in tumour cells and tumour-associated endothelial cells. The effects were pronounced when mice were treated with the combination of Glivec and taxol. Interestingly, immunohistochemical studies showed that tumour cells growing in the bone (but not those in surrounding musculature) expressed high levels of PDGF- α , PDGF- β , PDGFR- α and PDGFR- β . Tumour-associated endothelial cells within the bone also expressed PDGFR- α and PDGFR- β . These data indicate that inhibition of the PDGFR in combination with chemotherapy might provide a new approach for the treatment of bone metastasis.

Conclusion

The discovery and development of Glivec has shown that it is possible to produce rationally designed, molecular-targeted drugs for the treatment of a specific cancer. The research programme has also clearly shown that it is possible to define *in vitro* and animal models with high predictive quality, as the results of the subsequent clinical studies have largely corroborated the preclinical findings. The predictive quality was achieved in this particular case by using models with identical genetic abnormalities as those found in man. The case of Glivec also shows that compounds that do not only affect one, but two or more targets (which is frequently the case), can be beneficial in allowing several diseases with differing molecular abnormalities to be addressed, without paying too high a price in terms of toxicity.

The clinical data available so far in CML, GIST and chronic myeloproliferative disorders that involve rearrangement of the PDGFR gene indicate that the inhibition of BCR-ABL, c-KIT and PDGFRs can be achieved with Glivec in humans, and translated into clinically meaningful patient benefit. Providing clinical 'proof of concept', these data validate the initial hypothesis of this programme, and underscore the importance of rationally selecting the target diseases to be considered in the early phases of development of a molecule such as Glivec.

Beyond these reasonably well-understood malignancies, Glivec could have potential in the treatment of other malignancies that involve any of these signalling

pathways, or through targeting of the tumour micro-environment. However, most human cancers are likely to be heterogeneous with regard to molecular abnormalities, such as oncogene activation, and involve multiple signalling pathways in addition to either c-KIT and/or the PDGFR. Consequently, careful attention will have to be paid in designing clinical trials in these more complex indications as to how patients should be selected on the basis of the expression or activation of the molecular target in their tumour, as

far as is technically feasible. This point has been crucial in the successful outcome of the CML, GIST and CMML trials. The activity of Glivec in more common cancers with multiple and more complex molecular abnormalities remains to be determined, and is the objective of continuing research in diseases such as SCLC, prostate cancer and gliomas. The potential activity of the combination of Glivec with other signal-transduction inhibitors or anticancer agents is also being investigated.

1. Rowley, J. D. A new consistent abnormality in chronic myelogenous leukaemia identified by quinacrine fluorescence and giemsa staining. *Nature* **243**, 290-293 (1973).
2. Nowell, P. C. & Hungerford, D. A. A minute chromosome in human chronic granulocytic leukemia. *Science* **132**, 1497 (1960).
3. Daley, G. Q., Van Etten, R. A. & Baltimore, D. Induction of chronic myelogenous leukemia in mice by the p210^{bcr/abl} gene of the Philadelphia chromosome. *Science* **247**, 824-830 (1990).
4. Kellier, M. A. et al. Induction of chronic myelogenous leukemia in mice by the v-Abl and Bcr/Abl. *Proc. Natl Acad. Sci. USA* **87**, 6649-6653 (1990).
5. Heisterkamp, N. et al. Acute leukaemia in Bcr/Abl transgenic mice. *Nature* **344**, 251-253 (1990).
6. Lugo, T. G. et al. Tyrosine kinase activity and transformation potency of Bcr-Abl oncogene products. *Science* **247**, 1079-1082 (1990).
7. Lipinsky, C. A. Drug-like properties and the causes of poor solubility and poor permeability. *J. Pharmacol. Toxicol. Methods* **44**, 235-249 (2001).
8. Teague, S. et al. The design of leadlike combinatorial libraries. *Angew. Chem. Int. Edn Eng.* **38**, 3743-3748 (1999).
9. Zimmermann, J. et al. (Phenylamino)pyrimidine (PAP) derivatives: a new class of potent and highly selective PDGF-receptor autophosphorylation inhibitors. *Bioorg. Med. Chem. Lett.* **6**, 1221-1226 (1996).
10. Zimmermann, J. et al. Potent and selective inhibitors of the ABL-kinase: phenylamino pyrimidine (PAP) derivatives. *Bioorg. Med. Chem. Lett.* **7**, 187-192 (1997).
11. Zimmerman, J., Furet, P. & Buchdunger, E. STI571. A new treatment modality for CML. *ACS Symp. Ser.* **796**, 245-259 (2001).
12. Schindler, T. et al. Structural mechanism for STI571 inhibition of Abelson tyrosine kinase. *Science* **289**, 1938-1942 (2000).
The first description of the structural interactions between Glivec and ABL using crystallographic studies. Provided an important insight into potential mechanisms of resistance.
13. Okuda, K. et al. ARG tyrosine kinase activity is inhibited by STI571. *Blood* **97**, 2440-2448 (2001).
14. Druker, B. J. et al. Effects of a selective inhibitor of the Abl tyrosine kinase on the growth of Bcr-Abl positive cells. *Nature Med.* **2**, 561-566 (1996).
The first study to document the strong efficacy of Glivec in vitro and in vivo models of BCR-ABL-positive leukaemias.
15. Campi, M. et al. CGP 57148, a tyrosine kinase inhibitor, inhibits the growth of cells expressing BCR-ABL, TEL-ABL, and TEL-PDGFR fusion proteins. *Blood* **90**, 4947-4952 (1997).
16. Beran, M. et al. Selective inhibition of cell proliferation and BCR-ABL phosphorylation in acute lymphoblastic leukemia cells expressing M, 190,000 BCR-ABL protein by a tyrosine kinase inhibitor (CGP 57148). *Clin. Cancer Res.* **4**, 1661-1672 (1998).
17. Gambacorti-Passerini, C. et al. Inhibition of the ABL kinase activity blocks the proliferation of BCR/ABL⁺ leukemic cells and induces apoptosis. *Blood Cells Mol. Dis.* **23**, 380-394 (1997).
18. Deininger, M. et al. The tyrosine kinase inhibitor CGP57148B selectively inhibits the growth of BCR-ABL-positive cells. *Blood* **90**, 3691-3698 (1997).
19. Dan, S., Naito, M. & Tsunro, T. Selective induction of apoptosis in Philadelphia chromosome-positive chronic myelogenous leukemia cells by an inhibitor of BCR-ABL tyrosine kinase, CGP 57148B. *Cell Death Differ.* **5**, 710-715 (1998).
20. Le Coutre, P. et al. In vivo eradication of human BCR/ABL-positive leukemia cells with an ABL kinase inhibitor. *J. Natl Cancer Inst.* **91**, 163-168 (1999).
21. Wolff, N. C. & Iaria, R. L. Establishment of a murine model for therapy-treated chronic myelogenous leukemia using the tyrosine kinase inhibitor STI571. *Blood* **98**, 2808-2816 (2001).
22. Sliab, C. et al. STAT5 activation contributes to growth and viability in Bcr/Abl-transformed cells. *Blood* **95**, 2118-2125 (2000).
23. Horta, M. et al. Blockade of the Bcr-Abl kinase activity induces apoptosis of chronic myeloid leukemia cells by suppressing signal transducer and activator of transcription 5-dependent expression of BCL-X_L. *J. Exp. Med.* **191**, 977-984 (2000).
24. Oda, T. et al. Crkl is the major tyrosine-phosphorylated protein in neutrophils from patients with chronic myelogenous leukemia. *J. Biol. Chem.* **269**, 22925-22928 (1994).
25. Jonuleit, T. et al. Bcr-Abl kinase downregulates cyclin-dependent kinase inhibitor p27 in human and murine cell lines. *Blood* **96**, 1933-1939 (2000).
26. Gesbert, F. et al. BCR/ABL regulates expression of the cyclin dependent kinase inhibitor p27Kip1 through the PI3K/AKT pathway. *J. Biol. Chem.* **275**, 39223-39230 (2000).
27. Gaston, I. et al. Abl kinase but not PI3-kinase links to the cytoskeletal defects in Bcr-Abl transformed cells. *Exp. Hematol.* **28**, 77-86 (2000).
28. Druker, B. J. et al. Activity of a specific inhibitor of the BCR-ABL tyrosine kinase in the blast crisis of chronic myeloid leukemia and acute lymphoblastic leukemia with the Philadelphia chromosome. *N. Engl. J. Med.* **344**, 1038-1042 (2001).
The first clinical results with Glivec in CML, documenting a high level of efficacy, low level of toxicity and describing the dose-response relationship. These results confirm the crucial role of BCR-ABL in the pathophysiology of CML.
29. Druker, B. J. et al. Efficacy and safety of a specific inhibitor of the BCR-ABL tyrosine kinase in chronic myeloid leukemia. *N. Engl. J. Med.* **344**, 1031-1037 (2001).
30. Peng, B. et al. Clinical investigation of the PK/PD relationship for Glivec (STI571): a novel inhibitor of signal transduction. *Proc. Am. Soc. Clin. Oncol.* **20**, 280 (2001).
31. Kantarjian, H. et al. Hematologic and cytogenetic responses to imatinib mesylate in chronic myelogenous leukemia. *N. Engl. J. Med.* **346**, 645-652 (2002).
32. Talpaz, M. et al. GlivecTM (imatinib mesylate) induces durable hematologic and cytogenetic responses in patients with accelerated phase chronic myeloid leukemia: results of a Phase 2 study. *Blood* **99**, 1928-1937 (2002).
33. Sawyers, C. et al. Imatinib induces hematologic and cytogenetic responses in patients with chronic myeloid leukemia in myeloid blast crisis: results of a Phase II study. *Blood* **99**, 3530-3539 (2002).
34. Weisberg, E. & Griffin, J. Mechanism of resistance to the Abl tyrosine kinase inhibitor STI571 in BCR/ABL transformed hematopoietic cell lines. *Blood* **95**, 3498-3505 (2000).
35. Mahon, F. et al. Selection and characterization of BCR-ABL positive cell lines with differential sensitivity to the tyrosine kinase inhibitor STI571: diverse mechanisms of resistance. *Blood* **96**, 1070-1079 (2000).
36. Le Coutre, P. et al. Induction of resistance to the Abelson inhibitor STI571 in human leukemic cells through gene amplification. *Blood* **95**, 1758-1766 (2000).
37. Gorre, M. E. et al. Clinical resistance to STI-571 cancer therapy caused by BCR-ABL gene mutation or amplification. *Science* **293**, 876-880 (2001).
This study describes potential mechanisms of resistance in CML in clinical samples from treated patients.
38. Gorre, M. E. et al. Roots of clinical resistance to STI-571 cancer therapy. *Science* **293**, 2163a (2001).
39. Barthe, C. et al. Roots of clinical resistance to STI-571 cancer therapy. *Science* **293**, 2163a (2001).
40. Hochhaus, A. et al. Roots of clinical resistance to STI-571 cancer therapy. *Science* **293**, 2163a (2001).
41. Von Bubnoff, N. et al. BCR-ABL gene mutations in relation to clinical resistance of Philadelphia-chromosome-positive leukaemia to STI571: a prospective study. *Lancet* **359**, 487-491 (2002).
42. Manley, P. W. et al. Molecular interactions between GleevecTM and isoforms of the c-Abl kinase. *Proc. Am. Assoc. Cancer Res.* **4196** (2002).
43. Gambacorti-Passerini, C. et al. $\alpha 1$ Acidic glycoprotein (AGP) binds, inhibits and causes in vitro resistance of human BCR-ABL⁺ leukemic cells to STI571. *J. Natl Cancer Inst.* **92**, 1641-1650 (2000).
44. Jorgensen, H. G. et al. α -Acid glycoprotein expressed in the plasma of chronic myeloid leukemia patients does not mediate significant in vitro resistance to STI571. *Blood* **99**, 713-715 (2002).
45. Hofmann, W. K. et al. Relation between resistance of Philadelphia-chromosome-positive acute lymphoblastic leukaemia to the tyrosine kinase inhibitor STI571 and gene-expression profiles: a gene-expression study. *Lancet* **359**, 481-486 (2002).
46. Druker, B. STI571 (Gleevec/Glivec, imatinib) versus interferon (IFN) γ cytarabine as initial therapy for patients with CML: results of a randomized study. *Proc. Am. Soc. Clin. Oncol.* **1** (2002).
47. Buchdunger, E. et al. The Abl protein-tyrosine kinase inhibitor, STI571, inhibits in vitro signal transduction mediated by c-KIT and PDGF receptors. *J. Pharmacol. Exp. Ther.* **295**, 139-145 (2000).
48. Heinrich, M. C. et al. Inhibition of c-kit receptor tyrosine kinase activity by STI571, a selective tyrosine kinase inhibitor. *Blood* **98**, 925-932 (2000).
49. Hirota, S. et al. Gain of function mutations of c-KIT in human gastrointestinal stromal tumors. *Science* **279**, 577-580 (1998).
This study establishes the importance of c-KIT signalling in the pathogenesis of GIST tumours.
50. Lasota, J. et al. Mutations in exons 9 and 13 of *KIT* gene are rare events in gastrointestinal stromal tumors. A study of two hundred cases. *Am. J. Pathol.* **157**, 1091-1095 (2000).
51. Lux, M. L. et al. Kit extracellular and kinase domain mutations in gastrointestinal stromal tumors. *Am. J. Pathol.* **156**, 791-795 (2000).
52. Rubin, B. P. et al. Kit activation is a ubiquitous feature of gastrointestinal stromal tumors. *Cancer Res.* **61**, 8118-8121 (2001).
53. Heinrich, M. C. et al. STI571 inhibits the kinase activity of wild type and juxtamembrane c-KIT mutants but not the exon 17 D816V mutations associated with mastocytosis. *Blood* **96**, 4459 (2000).
54. Tuveson, D. A. et al. STI571 inactivation of the gastrointestinal stromal tumor c-KIT oncoprotein: biological and clinical implications. *Oncogene* **20**, 5054-5058 (2001).
55. Joensuu, H. et al. Effect of the tyrosine kinase inhibitor STI571 in a patient with metastatic gastrointestinal stromal tumor. *N. Engl. J. Med.* **344**, 1052-1056 (2001).
A proof-of-concept report of the efficacy of Glivec in KIT-expressing GIST, and rationale for further development in this indication, as well as in other solid tumours that express KIT.
56. Van Oosterom, A. T. et al. Safety and efficacy of imatinib (STI571) in metastatic gastrointestinal stromal tumors: a phase I study. *Lancet* **358**, 1421-1423 (2001).

57. Blanke, C. D. *et al.* Evaluation of the safety and efficacy of an oral molecularly-targeted therapy, STI571, in patients with unresectable or metastatic gastrointestinal stromal tumors (GISTs) expressing c-KIT (CD117). *Proc. Am. Soc. Clin. Oncol.* 20, 1 (2001).
58. Heinrich, M. C. *et al.* Inhibition of Kit kinase activity: a novel molecular approach to the treatment of Kit-positive malignancies. *J. Clin. Oncol.* 20, 1692–1703 (2002).
An excellent review of KIT as a target for anticancer therapy.
59. Krystal, G. W., Hines, S. & Organ, C. Autocrine growth of small cell lung cancer mediated by co-expression of c-kit and stem cell factor. *Cancer Res.* 56, 370–376 (1996).
60. Krystal, G. W., Carlson, P. & Litz, J. Induction of apoptosis and inhibition of small cell lung cancer growth by the quinazoline tyrostopostins. *Cancer Res.* 57, 2203–2208 (1997).
61. Krystal, G. W. *et al.* The selective tyrosine kinase inhibitor STI571 inhibits small cell lung cancer growth. *Clin. Cancer Res.* 6, 3319–3326 (2000).
62. Wang, W. L. *et al.* Growth inhibition and modulation of kinase pathways of small cell lung cancer lines by the novel tyrosine kinase inhibitor STI571. *Oncogene* 19, 3521–3528 (2000).
63. Buchdunger, E. *et al.* Effects of a selective inhibitor of the Abl tyrosine-kinase *in vitro* and *in vivo* by a 2-phenylaminopyrimidine derivative. *Cancer Res.* 56, 100–104 (1996).
64. Östman, A. & Heldin, C. H. Involvement of platelet-derived growth factor in disease: development of specific antagonists. *Adv. Cancer Res.* 80, 1–38 (2001).
65. Nistér, M. *et al.* Differential expression of platelet-derived growth factor receptors in human malignant glioma cell lines. *J. Biol. Chem.* 266, 16755–16763 (1991).
66. Klic, T. *et al.* Intracranial inhibition of platelet-derived growth factor-mediated glioblastoma cell growth by an orally active kinase inhibitor of the 2-phenylaminopyrimidine class. *Cancer Res.* 60, 5143–5150 (2000).
67. Shimizu, A. *et al.* The dermatofibrosarcoma protuberans-associated collagen type 1 α /platelet-derived growth factor (PDGF) B-chain fusion gene generates a transforming protein that is processed to functional PDGF-BB. *Cancer Res.* 59, 3719–3723 (1999).
68. Greco, A. *et al.* Growth inhibitory effect of STI571 on cells transformed by the COL1A/PDGF rearrangement. *Int. J. Cancer* 92, 354–360 (2001).
69. Sjöblom, T. *et al.* Growth inhibition of dermatofibrosarcoma protuberans tumors by the platelet-derived growth factor receptor antagonist STI571 through induction of apoptosis. *Cancer Res.* 61, 5778–5783 (2001).
70. Awan, R. A. *et al.* Patients with metastatic sarcoma arising from dermatofibrosarcoma protuberans (DFSP) may respond to imatinib (STI571, Gleevec). *Proc. Am. Soc. Clin. Oncol.* 1637 (2002).
71. Jousset, C. *et al.* A domain of TEL conserved in a subset of ETS proteins defines a specific oligomerization interface essential to the mitogenic properties of the TEL-PDGFR β oncoprotein. *EMBO J.* 16, 69–82 (1997).
72. Tomasson, M. H. *et al.* TEL/PDGFR β induces hematologic malignancies in mice that respond to a specific tyrosine kinase inhibitor. *Blood* 93, 1707–1714 (1999).
73. Apperley, J. F. *et al.* Chronic myeloproliferative diseases with t(5;12) and a PDGFRB fusion gene: complete cytogenetic remission with STI571. *Blood* 98, 726A (2001).
A proof-of-concept study of the efficacy of Gleevec in a PDGFR-driven malignancy.
74. Gulberg, D. *et al.* β 1 Integrin-mediated collagen gel contraction is stimulated by PDGF. *Exp. Cell Res.* 188, 264–272 (1990).
75. Rodt, S. A. *et al.* A novel physiologic role for platelet-derived growth factor-BB in rat dermis. *J. Physiol. (Lond.)* 495, 193–200 (1996).
76. Heuchel, R. *et al.* Platelet-derived growth factor receptor regulates interstitial fluid homeostasis through phosphatidylinositol-3 kinase signaling. *Proc. Natl Acad. Sci. USA* 20, 11410–11415 (1999).
77. Jain, R. K. Delivery of molecular medicine to solid tumors. *Science* 271, 1079–1080 (1996).
78. Pietras, K. *et al.* Inhibition of platelet-derived growth factor receptors reduces interstitial hypertension and increases transcapillary transport in tumors. *Cancer Res.* 61, 2929–2934 (2001).
79. Hellström, M. *et al.* Role of PDGF-B and PDGFR- β in recruitment of vascular smooth muscle cells and pericytes during embryonic blood vessel formation in the mouse. *Exp. Cell Res.* 186, 264–272 (1999).
80. Reinmuth, N. *et al.* Induction of VEGF in perivascular cells defines a potential paracrine mechanism for endothelial cell survival. *FASEB J.* 15, 1239–1241 (2001).
81. Wang, D. *et al.* Induction of vascular endothelial growth factor expression in endothelial cells by platelet-derived growth factor through the activation of phosphatidylinositol 3-kinase. *Cancer Res.* 59, 1464–1472 (1999).
82. Buchdunger, E., O'Reilly, T. & Wood, J. Pharmacology of imatinib (STI571). *Eur. J. Cancer* (in the press).
83. Uehara, H. *et al.* Blockade of PDGF-R signaling by STI571 inhibits angiogenesis and growth of human prostate cancer cells in the bone of nude mice. *Proc. Am. Assoc. Cancer Res.* 2192 (2001).

Acknowledgements

We would like to thank the members of the Gleevec International Project Team for their crucial contribution to the success of this programme and their kind review of this manuscript: P. Boutbee, V. Buss, S. Dimitrijevic, A. Dortok, D. Filipovic, I. Gathmann, H. Godman, J. Jaffe, L. Letvak, P. Marbach, R. Miranda, J. Ogorka, C. Ogawa, B. Peng, S. Silbermann, F. Sutter, S. Szabo, S. Wells and J. M. Ford. We also thank B. Druker for his crucial input and a fruitful collaboration throughout this programme, and N. Lydon for his contribution in the early phase of the programme. We thank also C. Schmid for her assistance in editing the manuscript.

Online links

DATABASES

The following terms in this article are linked online to: Cancer.gov:

http://www.cancer.gov/cancer_information/
acute lymphoblastic leukaemia | acute myelogenous leukaemia | chronic myelogenous leukaemia | ovarian cancer | prostate cancer | small-cell lung cancer | testicular cancer
LocustLink:
<http://www.ncbi.nlm.nih.gov/LocusLink/>
ABL | Abi | AGP | AKT | albumin | ARG kinase | ATP5A1 | ATP5C1 | BAK1 | BCL-X | BCR | Bcr | bFGF | Bruton tyrosine kinase | COL1A1 | CRKL | EGF receptor | c-ERBB2 | ERK1 | ERK2 | FGF | c-FMS | v-fms | IGF-1 receptor | INK4B | insulin receptor | JAK2 | c-KIT | p27 | PDGF- α | PDGF- β | PDGFR- α | PDGFR- β | P-GP | PKC | SCF | v-SRC | STAT5 | TEL | VEGF
Medscape DrugInfo:
<http://promini.medscape.com/drugdb/search.asp>
cytarabine | Gleevec | interferon | taxol | verapamil

FURTHER INFORMATION

FDA: <http://www.fda.gov/default.htm>
Access to this interactive links box is free online.